Charge transport in manganites: Hopping conduction, the anomalous Hall effect, and universal scaling

Y. Lyanda-Geller,* S. H. Chun,† M. B. Salamon,‡ P. M. Goldbart,§ and P. D. Han
Department of Physics and Materials Research Laboratory, University of Illinois at Urbana-Champaign, Urbana, Illinois 61801

Y. Tomioka, A. Asamitsu, and Y. Tokura
Joint Research Center for Atomic Technology (JRCAT), Tsukuba 305, Japan
(Received 1 December 2000; published 20 April 2001)

The low-temperature Hall resistivity ρ_{xy} of $La_{2/3}A_{1/3}MnO_3$ single crystals (where *A* stands for Ca, Pb, and Ca, or Sr) can be separated into ordinary and anomalous contributions, giving rise to ordinary and anomalous Hall effects, respectively. However, no such decomposition is possible near the Curie temperature which, in these systems, is close to metal-to-insulator transition. Rather, for all of these compounds and to a good approximation, the ρ_{xy} data at various temperatures and magnetic fields collapse (up to an overall scale), on to a single function of the reduced magnetization $m \equiv M/M_{\rm sat}$, the extremum of this function lying at $m \approx 0.4$. A mechanism for the anomalous Hall effect in the inelastic hopping regime, which reproduces these scaling curves, is identified. This mechanism, which is an extension of Holstein's model for the ordinary Hall effect in the hopping regime, arises from the combined effects of the double-exchange-induced quantal phase in triads of Mn ions and spin-orbit interactions. We identify processes that lead to the anomalous Hall effect for localized carriers and, along the way, analyze issues of quantum interference in the presence of phonon-assisted hopping. Our results suggest that, near the ferromagnet-to-paramagnet transition, it is appropriate to describe transport in manganites in terms of carrier hopping between states that are localized due to the combined effect of magnetic and nonmagnetic disorder. We attribute the qualitative variations in resistivity characteristics across manganite compounds to the differing strengths of their carrier self-trapping, and conclude that both disorder-induced localization and self-trapping effects are important for transport.

DOI: 10.1103/PhysRevB.63.184426 PACS number(s): 75.30.Vn, 72.20.My, 03.65.Ta

I. INTRODUCTION AND OVERVIEW

Numerous recent studies have focused on the Hall effect in the family of doped manganese oxides $La_{1-x}A_xMnO_3$ (in which *A* stands for Ca, Sr or Pb), famous for its colossal magnetoresistance[1,2] (CMR) and accompanying ferromagnet-to-paramagnet (FP) and metal-insulator (MI) transitions.[3–12] Despite substantial variations in, e.g., the ferromagnet-to-paramagnet transition temperature T_C and residual resistivity across this manganite family, measurements of the Hall effect reveal unusual features in both their metallic and insulating regimes. An example of the Hall effect data is shown in Fig. 1. In the metallic state the Hall (i.e., transverse) resistivity ρ_{xy} at lowest temperatures (curve at 10 K in Fig. 1) exhibit just the ordinary Hall effect (OHE), proportional to the external magnetic field *B*. At higher temperatures in the metallic phase, the Hall resistivity can be separated into the sum of (i) a (positive) ordinary Hall effect, and (ii) a (negative) anomalous Hall effect (AHE), proportional to the magnetization *M*, as shown for the curve at 200 K on Fig. 1. The effective density of carrier holes, as deduced from the slope of OH resistivity, is typically found to be several times larger than that set by the nominal doping level.

This difference has been attributed to the effects of charge compensation and Fermi-surface shape.[9] The AHE is commonly observed in ferromagnets, but the sign and the magnitude of the AHE in manganites stand in contradiction to conventional theories based on skew-scattering[13–16] or side-jump processes.[15,17–19] Most striking is the rapid increase in the prominence of the AHE that occurs at temperatures *T* close to T_C. In this range of temperatures, ρ_{xy} can no longer be simply separated into ordinary and anomalous parts, as can be seen from the curve at 300 K in Fig. 1. For temperatures well above T_C, ρ_{xy} again becomes linear in *B*, although its sign is now negative.[4–7,9,10,12] The corresponding Hall coefficient R_H ($\equiv \rho_{xy}/B$) decreases exponentially with increasing temperature in this regime, and a previous study identified a clear crossover from nonpolaronic to polaronic charge transport at around 1.4 T_C.[12]

The purpose of the present paper is to address the issue of charge-carrier motion in manganites, both experimentally and theoretically, focusing on the vicinity of the FP and MI transitions, from the vantage point afforded by the Hall effect. Our experimental results have led us to focus on the anomalous contribution to the Hall effect, and to develop a microscopic theoretical picture of the charge-carrier motion that gives rise to this contribution in manganites. The picture that emerges is one in which the essential character of charge-carrier motion is inelastic hopping between states localized due to magnetic and other sources of disorder.

In order to explain the Hall effect in the manganites in the vicinity of T_C, it is necessary to understand how the nature of the charge-carrier states are influenced by the magnetic order of the system. In this regard, the double-exchange interaction (DEI), which makes charge-carrier motion of Mn outer-shell carriers sensitive to magnetic alignment of core 3/2 spins of Mn ions (Hund rules lead to alignment of spins in three inner orbitals resulting in core spin 3/2), has long

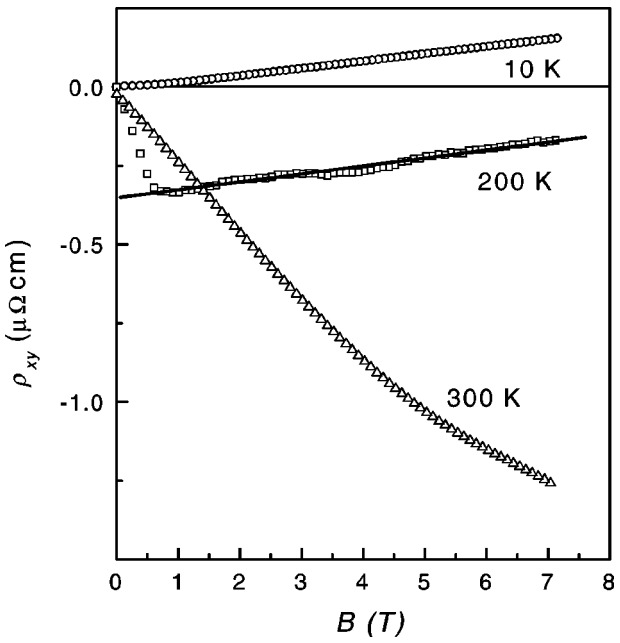

FIG. 1. Hall resistivity of manganites versus magnetic field for a selection of temperatures. At 10 K the Hall effect is *ordinary*; the slope extrapolates to the origin. At 200 K the Hall effect has both *ordinary* and *anomalous* components; the slope does not extrapolate to the origin, the offset signaling the anomalous Hall effect. At 300 K it is not simple to separate the Hall resistivity into *ordinary* and *anomalous* components.

been known to play a key role in transport in manganites, having been introduced by Zener[20] and elaborated by Anderson and Hasegawa[21] and De Gennes.[22] Therefore, our approach to exploration of the anomalous Hall effect in manganites is based on the picture of hopping conduction in the presence of double-exchange interaction.

A picture of the ordinary Hall effect in hopping conductors was developed long ago by Holstein,[23] in which the critical ingredient is the Aharonov-Bohm quantal phase[24] acquired as charge-carriers hop in the presence of magnetic field around closed sequences of localized states. The theoretical work reported here amounts to the generalization of Holstein's ideas suited to DE systems. The primary distinctions from Holstein's ideas are as follows: (i) Localization is now, to a great extent, caused by magnetic disorder in the orientation of core spins (and the attendant randomization of hopping amplitudes); the effects of magnetic disorder are facilitated by static disorder, and accompanied by polaronic effects. (ii) The relevant quantum-mechanical phases now arise via the quantal version of the Pancharatnam phase.[25,26] (iii) In order for a net Hall effect to result, account must be taken of Dzyaloshinskii-Moriya spin-orbit coupling.[27] The AHE mechanism that we propose arises in hopping regime in systems with localized states, and is the only possible microscopic mechanism of AHE in such systems. A brief account of this work was published in Refs. 10 and 11.

From the perspective of symmetry, it is well known that spin-orbit interactions lead to AHE.[13–19] The appreciation that a spin-generated geometric phase, in addition to spin-orbit interactions, is an essential ingredient for the development of a theory of the AHE in DE systems dates back to the 1998 manuscript of Kim, Majumdar, Millis, and Shraiman.[28] From the perspective of the microscopic mechanism of the AHE, both Ref. 28 and the paper of Ye *et al.*[29] that superceded it, invoke a field-theoretic scheme for integrating out the charge-carrier motion and, therefore, were intended mostly for metallic regimes (i.e., regimes in which charge transport occurs via *delocalized* states). Ye *et al.* have also addressed the polaron hopping regime by using high-temperature expansion.[30] By contrast, the present work considers the microscopic picture of nonmetallic regimes (i.e., regimes in which charge transport occurs via inelastically-assisted hopping between *localized* states). Elsewhere, we shall address the issue of the microscopic mechanism of the AHE in the metallic regime.[31]

The microscopic mechanism of AHE that we propose for systems with localized states leads to remarkable prediction: the Hall resistivity ρ_{xy} depends on the temperature and the magnetic field solely through the magnetization M, i.e., $\rho_{xy} = \rho_{xy}(M(H,T))$. This universal scaling has been observed experimentally in manganites. Here, we provide a detailed discussion of our theoretical picture of hopping transport in manganites. Further, the present paper reports on measurements made on additional compounds having lower and higher transition temperatures and provides an analysis of these data in terms of our theoretical picture.[10,11] The universal scaling relation between ρ_{xy} and M reported for is shown to hold for the manganese oxides $La_{2/3}Ca_{1/3}MnO_3$ (LCMO), $La_{2/3}Sr_{1/3}MnO_3$ (LSMO), and $La_{2/3}Ca_{1/9}Pb_{2/9}MnO_3$ (LPMO). Although data on the Hall effect in these compounds have universal features, the temperature dependence of resistivity in LSMO is different from that in LCMO and LPMO. This behavior is due to different size of dopant ions which results in different static disorder, different carrier localization length, and, accordingly, different strength of self-trapping due to lattice effects. We believe that the accuracy of the results concerning the AHE based on inelastic charge-carrier hopping between states localized due to magnetic and nonmagnetic sources of disorder suggests that the dominant mechanism for charge transport in the transition regime is indeed inelastic charge-carrier hopping between localized states, which differs qualitatively from the picture of metallic conduction perturbed by double-exchange interactions. As for polaronic effects, depending on the compound, they may set in soon as localization length is of the order of lattice constant. These effects (or their absence) are crucial for the character of the temperature behavior in the range of high temperatures above the FP and MI transitions. Polaronic effects do not affect the universal scaling of the anomalous Hall resistivity. At the same time, scaling of the AH resistivity of the type observed in the CMR regime is not contained in conventional models of the AHE in the metals (i.e., those based on skew-scattering and side-jump mechanisms). Neither is this scaling contained in a Berry phase mechanism for the AHE in the metallic phase, discussed in Refs. 28 and 29. We regard this as further evidence against the viability of any metallic-based picture of transport in the transition regime.

How does the present work relate to earlier work on charge transport in the CMR regime? Attempting to build on the early key insight that DE plays a central role, Millis

et al.[32] considered transport in DE systems within the framework of the coherent potential approximation (CPA). Making the CPA in the present context amounts to replacing the charge and magnetic system by an effective one, involving only the charge subsystem, in which the conduction band width depends on the magnetization but there is no other effect of the magnetic sector. Thus, any resistivity obtained via such a scheme is simply whatever the resistivity of the charge sector was, reduced by an extent that depends on the magnetic order via a renormalization of the bandwidth. The picture enforced by this approach is that the fundamental mechanism for charge transport is metallic in nature. Naturally, the CPA approach[32] is unable to yield a colossal magnetoresistance, although it can provide factors on the order of unity. What it explicitly omits is any resistivity mechanism arising from localization due to magnetic disorder, as noted by Varma.[33] Rather than appeal to such a localization process, Millis *et al.*[34] proposed that the magnetization-dependent reduction of the bandwidth invites lattice effects. Specifically, the (now magnetically) heavy charge carriers would be more susceptible to self-trapping by a large Jahn-Teller lattice distortion, which would cause a metal-insulator transition via polaronic collapse of the conduction bandwidth.

Accepting, for the moment, the notion that charge transport in the transition regime is indeed accomplished by lattice polarons, let us ask what the consequences would be for the resistivity. According to theory of polaronic transport, developed in series of papers in 1960s by Holstein alone,[35] with Friedman[36] and with Emin,[37] polaronic-type conduction manifests itself via a specific temperature-dependence of the longitudinal and Hall resistivities, being activated in character with a definite relationship between the activation constants for these resistivities. Following the proposal of polaronic-type conduction by Millis *et al.*, experimental tests of these temperature dependences were performed. Initial results[4] in LPMO over the range of temperatures high above the MI and FP transitions seemed in accordance with the polaronic picture. However, recent extensive measurements at lower temperatures, in transition regime,[12] demonstrate that, at least in this regime, the temperature dependence of the longitudinal and Hall resistivities cannot be explained in terms of polaronic picture alone. Furthermore, even at high temperatures, polaron-based picture is not compatible with experimental data for LSMO samples.

With the pictures of charge transport in the CMR regime based on either the magnetization-dependent reduction of the bandwidth or on polarons alone invalidated, what remains is the possibility of constructing a valid picture based on nonpolaronic localization of charge carriers. Strong evidence supporting such a picture comes from a simple estimate of the scattering time (i.e., the scattering-induced conduction-band broadening), which indicates that, in the transition regime, the band broadening exceeds the band width (i.e., the mean free path is shorter than the Fermi wavelength) so that the resistivity exceeds the Mott-Ioffe-Regel limit and, hence, the conduction cannot be metallic. Therefore, one needs to search for insulating transport mechanisms and, specifically, the origins of carrier localization that are distinct from polaronic effects. (We note that in compounds in which the Jahn-Teller distortion is not symmetry-allowed, this is especially important.) Such localization can result from both magnetic disorder (i.e., due to lack of core-spin alignment) and non-magnetic disorder (i.e., static potential disorder due, e.g., to doping).[38]

While the localizing influence of nonmagnetic disorder on charge transport has been thoroughly investigated,[39,40] the influence of magnetic disorder is less well known, and we shall discuss it in detail in Sec. III B. For now, we simply mention that the magnetic disorder in core 3/2 spin orientation experienced by the outer-shell charge carriers arises via the DE interaction from fluctuations around the ferromagnetic state that build up as the FP transition is approached from the low temperature side. Of course, these fluctuations are dynamical, but they are slow, compared with characteristic timescales for outer-shell charge-carrier motion. Thus, for the purposes of analyzing the influence of the magnetic sector on charge transport, it is appropriate to regard orientations of the core spins on the Mn ions as quenched variables. The resulting magnetic disorder takes the form of randomness in the off-diagonal hopping matrix elements for the charge carriers. By contrast, nonmagnetic disorder occurs due to randomness in the substitution of La by dopant ions (e.g., Sr, Pb, or Ca), and gives rise to the more familiar diagonal (Anderson-type) disorder. Electronic states in systems with off-diagonal disorder were first considered by Lifshitz,[41] who showed that localized states arise in the band tail. The physical picture of carrier states in manganites must encompass both magnetic and nonmagnetic disorder, possibly facilitated by Coulomb effects, which (jointly or severally) can result in carrier localization.

If carriers are localized then they can still participate in transport, but it is by hopping from one localized state to another, assisted by one or more inelastic agents (such as phonons). In this case, the longitudinal resistivity is determined by the rate of inelastic hopping between occupied and unoccupied states.[39,42] When carrier localization has occurred, and the localization length is of order of lattice constant, electronic interaction with lattice and self-trapping effects can become essential, so that at high temperature resistivity is determined by small polarons. However, transitional regime is greatly affected by carrier localization of nonpolaronic origin. We notice that in general one should distinguish between Jahn-Teller polarons and Holstein breathing mode polarons: the presence of the former depends on symmetry of the system, the latter arise independent of the underlying symmetry. In manganites, both types of polarons are capable of facilitating carrier localization by magnetic and nonmagnetic disorder; when carriers are localized on lattice constant scale, Holstein polarons govern the temperature dependence of resistivity deep in the insulating phase.

In the present paper, we shall not consider metallic manganites, and restrict our consideration to the inelastic hopping transport regime. The discussion of the Hall effect in metallic ferromagnets will be presented elsewhere.[31] The present paper is organized as follows. In Sec. II we describe the experimental setup and in Sec. II B we present experi-

mental data on the longitudinal resistivity, magnetization and Hall resistivity in three different manganite compounds having distinct transition temperatures. Section III is organized into several subsections, in which we describe models of disorder in manganites, issues related to the localization of carriers and the hopping transport mechanism, as well as the quantal Pancharatnam phase, spin-orbit Dzyaloshinski-Moriya interactions, and the universal scaling of the Hall resistivity. In Sec. IV we discuss the correspondence between our theoretical and experimental results.

II. EXPERIMENTS ON TRANSPORT AND MAGNETIC PROPERTIES OF MANGANITES

A. Experimental method

In the experimental part of this study, single crystals of various manganites were used in order to avoid extrinsic effects from grain boundaries or strains. In single crystals, simultaneous measurements of transport and magnetic properties permits us to find a precise dependence of transport coefficients on the sample magnetization. We have measured the longitudinal and Hall resistivities and the magnetization of three different crystals with various transition temperatures. $La_{0.7}Ca_{0.3}MnO_3$ (LCMO) and $La_{0.7}Sr_{0.3}MnO_3$ (LSMO) single crystals were prepared by the floating-zone method. $La_{0.67}(Ca,Pb)_{0.33}MnO_3$ (LPMO) single crystals were grown from 50/50 PbF_2/PbO flux. More details on the sample growth and basic properties can be found elsewhere.[43,44] All specimens used in the measurements were cut along crystalline axes into bar shapes from larger pre-oriented crystals. Contact pads for Hall resistivity measurements were made by sputtering $\approx$1500 Å of gold through a mask. Gold wires of 50 μm diameter are then attached using slowly drying silver paints. Typical contact resistances after annealing were about 1 Ω at room temperature. We adopted a low-frequency (39 Hz) ac method for the measurements. The transverse voltage signal was first nulled at zero field at each temperature below 400 K by a potentiometer, and the change in the transverse voltage was recorded as H was swept from $+7$ T to -7 T and back for averaging. Following the transport measurements, sample magnetizations were measured by a 7 T SQUID magnetometer on the same samples.

B. Experimental results

Figure 2 shows the temperature dependences of magnetization measured at 1 T and 7 T. All three samples show ferromagnetic-to-paramagnetic phase transitions. The Curie temperatures T_C were determined by scaling analysis on high field $M(H)$ curves near the transition, and the results are shown in Table I. As T_C decreases, the transition becomes sharper, resulting in anomalous critical exponents.[45]

The temperature dependences of the longitudinal resistivities ρ_{xx} for the same set of samples under zero magnetic field and under 7 T are shown in Fig. 3. LCMO and LPMO show metal-insulator transitions near T_C, whereas LSMO shows an inflection at T_C, but ρ_{xx} continues to increase with increasing temperature above T_C. The metal-insulator transition temperatures T_{MI}, determined by the maximum in the rate of change in the temperature dependence of the longitudinal resistivity $d\rho_{xx}/dT$ under zero magnetic field, were slightly higher than corresponding T_C's (Table I). Also shown in Table I are ρ_{xx} minima (occurring at the lowest temperatures) and magnetoresistivity (MR) maxima [defined by $(\rho_{xx}(0\ \mathrm{T})-\rho_{xx}(7\ \mathrm{T}))/\rho_{xx}(7\ \mathrm{T})$]. The observed decrease in T_C correlates with the overall increases of resistivity and MR, which can be clearly seen in Fig. 3.

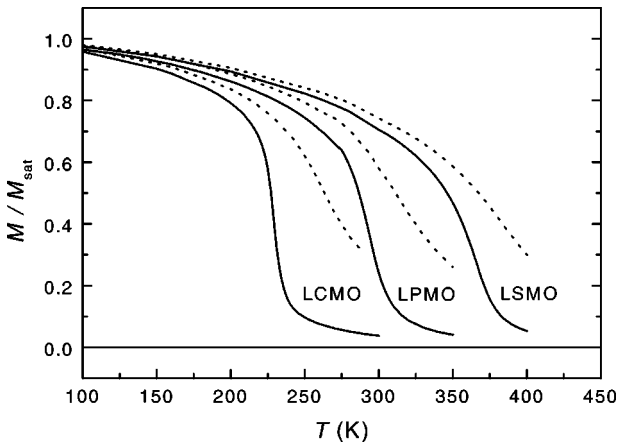

FIG. 2. Temperature dependences of normalized magnetization M/M_{sat} under 1 T (solid lines) and under 7 T (dotted lines) magnetic fields.

Despite differences in T_C, T_{MI} and temperature dependence of longitudinal resistivity across the three compounds, the Hall resistivity of compounds with doping that corresponds to maximal T_C show similar temperature and field dependences, as shown in Figs. 4, 5, and 6. At low temperatures, ρ_{xy} is positive and linear in magnetic field, the sign indicating holelike charge carriers, and negligible anomalous Hall contribution. As the temperature is increased, the high-field slope is roughly the same. However, the increasing, negative, contribution to ρ_{xy} shifts it downward. Quantitatively, ρ_{xy} can be expressed as a sum of an ordinary contribution parametrized by $R_0(T)$ and an anomalous contribution parametrized by $R_S(T)$ (Ref. 46):

$$\rho_{xy}(B,T)=R_0(T)B+\mu_0 R_S(T)M(H,T), \qquad (2.1)$$

where $B=\mu_0[H+(1-N)M]$, H is the external magnetic field, and $N\approx 1$ is the demagnetization factor. As has commonly been observed in manganite crystals and thin films, the effective charge-carrier density $n_{\mathrm{eff}}\equiv 1/eR_0$ is scattered between 1.0 and 2.4 holes/Mn (see Table I), which is much larger than the nominal doping level (of 0.3–0.33 holes/Mn), presumably due to the effects of the anisotropy of the Fermi surface.[9] We refer to our previous publications for the discussion on the low temperature OHE.[9]

On further increase of the temperature through T_C, ρ_{xy} becomes much larger, strongly curving with magnetic field, and the positive, high-magnetic-field contribution, linear in the field, which would arise from the ordinary Hall effect in a metallic phase due to the Lorentz force acting on charge-carriers, disappears. Owing to its low T_C, for the LCMO sample we were able to explore temperatures far above T_C,

TABLE I. Characteristics of single crystal samples used in this study.

	Composition	T_C	T_{MI}	min ρ_{xx}	max MR	n_{eff}(10 K)
LCMO	$La_{0.7}Ca_{0.3}MnO_3$	216.2 K	222.5 K	140 $\mu\Omega$ cm	2600%	1.6 holes/Mn
LPMO	$La_{0.67}(Ca,Pb)_{0.33}MnO_3$	285.1 K	287.5 K	91 $\mu\Omega$ cm	326%	2.4 holes/Mn
LSMO	$La_{0.7}Sr_{0.3}MnO_3$	359.1 K	362.0 K	55 $\mu\Omega$ cm	64%	1.0 holes/Mn

where ρ_{xy} shows a negative Hall coefficient, despite the doping of the material being by holes. In this range of temperatures the Hall coefficient $R_H=\rho_{xy}(B)/B$ exhibits activated behavior, with a characteristic energy $E_H\approx\frac{2}{3}E_\sigma$, where E_σ is the activation energy for ordinary conductivity σ_{xx}. Similar experimental results have been obtained in Refs. 4 and 12. In these works, investigations of manganite carrier-transport deep in the insulating phase have shown that the sign and temperature dependence of the high-temperature (i.e., above $1.4T_C$) Hall coefficient R_H ($\equiv\rho_{xy}/B$) can be explained in terms of the adiabatic hopping of small polarons.

Initially,[4] high-temperature transport picture due polaron hopping to was believed to support the proposal by Millis *et al.*[32] that the Jahn-Teller distortion which, according to symmetry considerations can occur in the MnO_6 octahedra of $LaMnO_3$, is responsible for the insulating behavior of doped $La_{1-x}A_xMnO_3$ systems. Hall resistivity measurements should be capable of providing key evidence for or against the polaronic picture of charge transport. According to the theory of this picture, the adiabatic hopping of small polarons[37] leads to an activation energy E_H characterizing R_H that is 2/3 of the activation energy E_ρ characterizing ρ_{xx},[37] as is observed at high temperatures.[4,12] However, recent Hall resistivity measurements, extending into the transition region[12] show that the activation energy changes abruptly at a crossover temperature $1.4T_C$, from the polaronic value of $\frac{2}{3}E_\sigma$ to a much larger value, $1.7E_\sigma$. This clearly marks the breakdown of the small polaron picture of charge transport, as shown in Fig. 4 (inset). In fact, the effective activation energy of the conductivity begins to decrease from a value of E_σ at roughly the same crossover temperature, making even greater the discrepancy between the experimental data and the small-polaron hopping picture. Even more dramatically, the product of the Hall mobility μ_H and the temperature, viz., $\mu_H T=-\sigma_{xx}R_H T$ which, according to the small polaron picture, should decrease monotonically with decreasing temperature, in fact is found to exhibit a minimum at the same crossover temperature. (We shall later show that, near T_C, ρ_{xy} is determined solely by the sample magnetization in all three compounds.) Thus, experiments in transition region lead to the conclusion that, while small polarons are an essential part of the physics of transport in manganites at high temperatures, they cannot provide a complete picture of the metal-to-insulator transition.

More generally, as discussed by Varma,[33] there exist double-exchange systems, such as $TmSe_xTe_{1-x}$, in which transport phenomena observed in manganese oxides are also observed but Jahn-Teller distortions, leading to small polarons, are not symmetry-allowed. At the same time, if the carrier localization length becomes of order of lattice constant, lattice effects in the form of Holstein breathing mode polarons arise naturally. This allows to explain why the high-temperature regime in some of manganese compounds exhibits longitudinal and Hall resistivities characterized by thermally-activated behavior which is qualitatively and quantitatively consistent with that caused by polaronic transport mechanism. Before turning to the theoretical picture of transport in manganites and, specifically, of AHE for localized carriers, we pause to examine whether the theoretical model of the AHE proposed by Ye *et al.*[29] which is based on

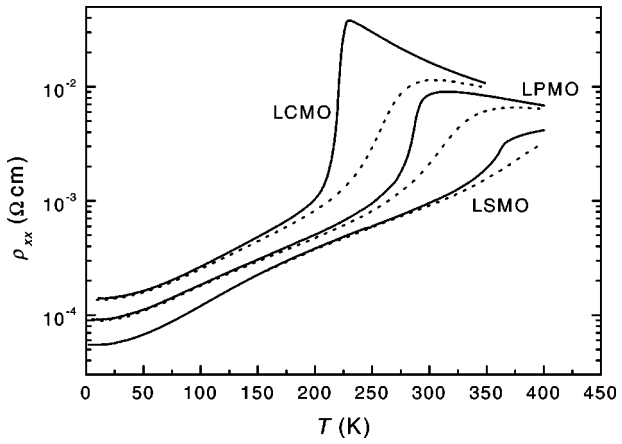

FIG. 3. Temperature dependences of longitudinal resistivity ρ_{xx} under zero magnetic field (solid lines) and under 7 T (dotted lines).

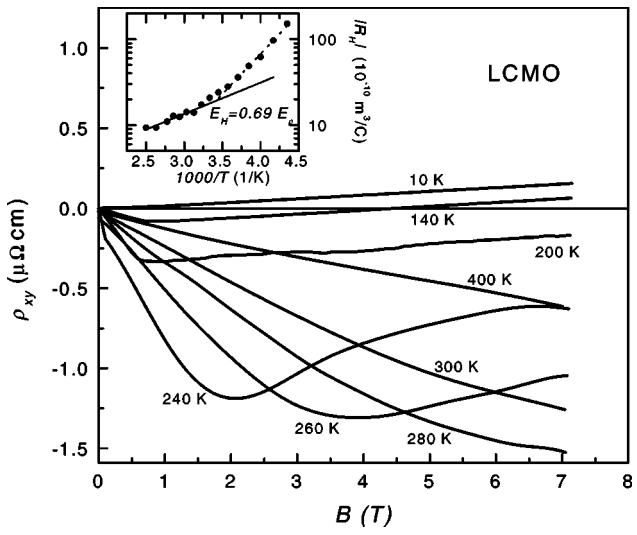

FIG. 4. Main panel: Hall resistivity ρ_{xy} of LCMO as a function of magnetic field at the indicated temperatures. Inset: Activated behavior of the high temperature Hall coefficient R_H.

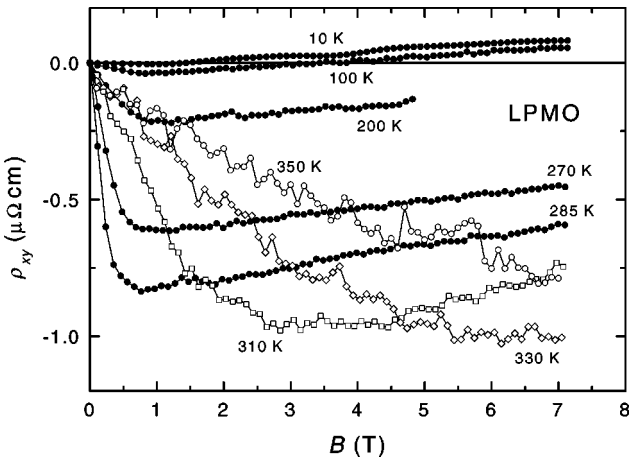

FIG. 5. Hall resistivity ρ_{xy} of LPMO as a function of magnetic field at the indicated temperatures.

a metallic view of charge transport, is consistent with our experimental data. In that model, following an earlier model by Kim *et al.*,[28] it is assumed that tight-binding charge carriers propagate coherently through a smoothly varying magnetization texture which has the effect of introducing a Berry phase gauge potential.[47–51] A central prediction of the model due to Ye *et al.* is that a peak should occur in $R_S(T)$ above T_C, along with a singularity in the slope at T_C, i.e., $dR_S/dT \sim |1-T/T_C|^{-\alpha}+c$, where α is the specific heat exponent. To test this prediction, we measured the low magnetic field (<0.5 T) magnetization and Hall resistivity of our most metallic sample, LSMO near T_C (see Fig. 7). From the behavior of ρ_{xy} and M in the zero-field limit, we determined $R_S \equiv (d\rho_{xy}/dM)$. In contrast to the prior report by Matl *et al.*[6], in this ''metal-to-metal'' transition system we do not find R_S to be proportional to ρ_{xx}. As seen on Fig. 7, ρ_{xx} flattens at the temperature at which the resistive transition is complete (i.e., $T_C^*=368$ K). This allows us to conclude that neither a constant R_S/ρ_{xx} nor a peak in R_S is a common feature in manganites. We note that close to T_C^*, it is possible to express $R_S(T)$ as a power law, $(1-T/T_C^*)^{0.82}$

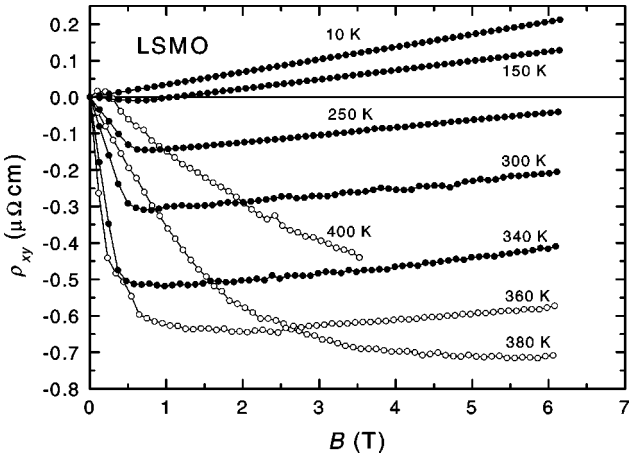

FIG. 6. Hall resistivity ρ_{xy} of LSMO as a function of magnetic field at the indicated temperatures.

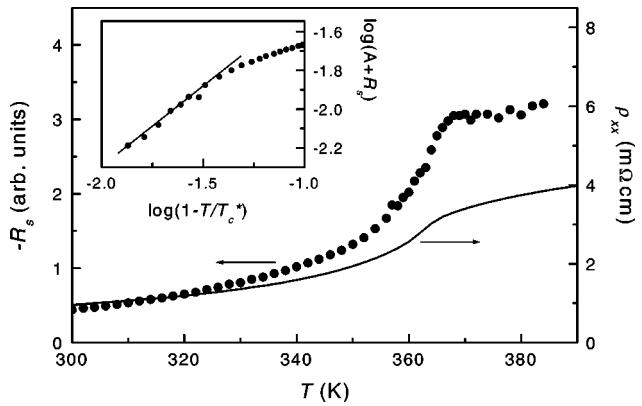

FIG. 7. Main panel: The anomalous Hall coefficient R_S (symbols) compared with the longitudinal resistivity ρ_{xx} (solid line). Inset: The critical behavior of R_S.

$+A$ (see Fig. 7, inset). However above $T_C^*=368$ K, which is significantly higher than both T_C and T_{MI} (see Table I), R_S is constant, and the fit does not correspond to the inflection point predicted in Ref. 29.

III. THEORY OF HOPPING MAGNETOTRANSPORT IN MANGANITES

The aim of the present section is to develop a picture of the Hall effect in manganites, to test this picture through comparison with experimental data and, hence, to build as completely as possible a general picture of the charge transport in manganites in the ferromagnet-to-paramagnet transition regime. Among the results we shall obtain, perhaps the most striking is the universal scaling of the magnetization-dependent Hall resistivity, which we explain should hold in the regime where charge transport proceeds primarily via hopping between localized states. Such universal scaling has been observed experimentally.

A. Disorder and interactions in manganites

Manganites are extremely complicated materials, and a bewildering variety of behaviors occurs in them, as the doping level, temperature or magnetic field is varied. Here, we focus on those manganites that exhibit a transition from a ferromagnetic metal to a paramagnetic insulator, controlled by temperature, as occurs in manganite compounds, doped with Ca or Sr or (Pb and Ca) substituting for La, at doping levels of around 1/3. This doping, of course, results in several sources of static disorder: (i) the dopant ions subsitute randomly for La; and (ii) the lattice distortion around the two ionizations of Mn (viz. Mn^{3+} and Mn^{4+}) is distinct (i.e., the breathing-mode effect). This disorder leads to local variations in the amplitudes for the hopping processes that carry charges between magnetic ions. Furthermore, (iii) any clustering of dopants in the randomly doped lattice would lead to fluctuations in the carrier density. These sources produce *nonmagnetic* disorder.

Along with the motion of charge carriers there is also the motion of core spins. In the present context, we believe that it is profitable to treat theses core spins classically, and to

regard the carrier dynamics as being much faster than the spin dynamics, so that the carrier motion can be pictured as taking place within a frozen core-spin configuration that is randomized owing to thermal fluctuations (i.e., we adopt a quasi-static approach). We term such random magnetic configurations ''magnetic disorder.'' We note that spin-spin correlation times have been obtained experimentally from muon spin relaxation and neutron spin echo data;[52] these experiments show that, indeed, spin dynamics is slow.

Strong thermal fluctuations render typical instantaneous configurations of the spins rather inhomogeneous. Among these fluctuations, there are the ''hedgehog'' excitations which, owing to their topological stability, are long-lived, and become more numerous as the ferromagnet-to-paramagnet transition is approached.[53] Due to the resulting magnetic inhomogeneity, the carrier-hopping matrix elements are reduced.

As we shall discuss in the following subsection, the presence of nonmagnetic and magnetic disorder both support the notion that the carrier states are localized at temperatures near to the (zero-magnetic-field) FP transition, as well as at higher temperatures. Such localization of carriers can explain the resistive transition which, in turn, leads to the disappearance of double-exchange-induced ferromagnetic spin-correlations, at least on spatial scales larger than the localization length. We note that in a series of papers[54] Furukawa has considered the issues of carrier states and transport in manganites by using a dynamical generalization of the coherent potential approximation, arriving at the conclusion that the transport properties of manganites can be explained in terms of the scattering of metallic carriers by magnetic randomness. We, however, believe that the fact that (in the range of temperatures marking the transition regime) the resistivity exceeds the Mott-Ioffe-Regel limit renders any approach founded on the scattering of delocalized carrier states to be inconsistent.

As discussed above in Sec. I, localization effects related to Jahn-Teller distortions and small-polaron formation cannot explain certain central experimental data in the transition regime, including the temperature dependence of both the resistivity and the Hall effect. Therefore, one is forced to consider alternative mechanisms that can lead to the breakdown of metallic conductivity and can also serve as an origin of various universal transport properties that have been observed in double-exchange systems, including, e.g., those in which Jahn-Teller distortions are symmetry-forbidden. For these reasons, we now give a discussion of the physics of disorder-induced carrier localization in manganites.

B. Disorder-induced carrier localization in manganites

To see why it is useful to regard charge transport as taking place in a frozen random background of core-spin orientations, let us imagine the spin configuration to be truly static. In the transition regime, a typical spin configuration is rather inhomogeneous and, hence, we expect carriers to be localized. Support for this notion comes from the close similarity between transport in manganites and systems of randomly located identical impurities (i.e., off-diagonal disorder). For the latter, localization has been established via the work of Lifshitz.[41] Although spin-induced randomness in manganites [arising from the random double-exchange factors of $\cos(\theta/2)$, where θ is the angle between core spins on Mn ions, see, e.g., Sec. III E] is weaker than the randomness considered in Ref. 41, we expect the two systems to exhibit qualitatively similar localization behavior. Furthermore, the condition for localization in the Lifshitz model (viz. that the characteristic spatial scale of the outer-shell wave functions in isolated Mn ions be much smaller than distance between sites) is well obeyed in manganites. Therefore, provided that there is appreciable randomness in the core-spin orientations, transport properties should be determined by the short-distance physics of clusters of ions and by magnetic correlations between such clusters. Moreover, nonmagnetic disorder and possible states bound to the subsituting *A*-site ions are capable of amplifying the trend towards localization.[33,38] In Fig. 8 we present a one-dimensional caricature of disorder in manganites, in which diagonal and off-diagonal disorder coexist. Sheng *et al.* included both magnetic and nonmagnetic disorder and applied one-parameter scaling theory[55] and finite-size scaling ideas[56] in order to investigate carrier localization in manganites numerically. Sheng *et al.* found that, in the presence of magnetic disorder, an Anderson metal-insulator transition accompanies the ferromagnet-to-paramagnet transition. They also observed an interesting correlation between T_C and the residual resistivity, which is determined by nonmagnetic disorder, viz., the larger the residual resistivity, the smaller the T_C; this agrees well with the original double-exchange picture, in which carrier motion promotes ferromagnetism whereas disorder resists electronic motion and, therefore, does not promote ferromagnetism.

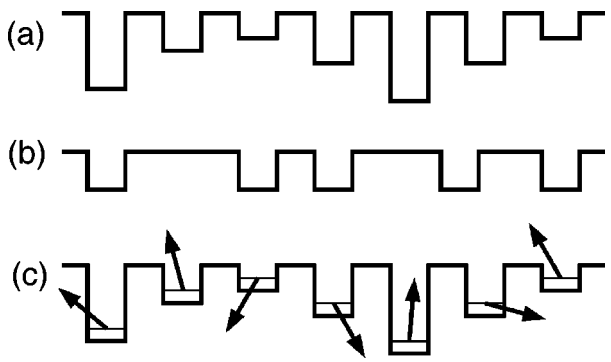

FIG. 8. Schematic one-dimensional picture of disorder in manganites. (a) Anderson model with on-site disorder; (b) Lifshitz model with random ionic locations (leading to random transfer integrals); (c) model of disorder in manganites, showing on-site disorder and magnetic disorder (leading to random transfer integrals).

To what extent can one regard charge transport as taking place in a frozen spin configuration? Equivalently, what are the characteristic time scales for magnetic and charge dynamics? For charge dynamics the time scale is $\hbar/t$, where t is a characteristic magnitude of the hopping matrix element, i.e., the shortest relevant time scale. For magnetic dynamics, the issue is more complicated. However, the shortest time scale is presumably $\hbar/k_B T$, which, in the regime of interest

to us, is greater than $\hbar/t$. Furthermore, as discussed by Lau and Dasgupta,[53] in three-dimensional magnetic systems the ferromagnet-to-paramagnet transition involves very long-lived topological excitations (i.e., magnetic hedgehogs)[57] which, as we shall see, are particularly significant for the AHE. Hence, we see that, to a first approximation, one can regard charge transport as taking place in a frozen spin configuration. Corrections to charge dynamics, due to magnetic dynamics (as well as feedback into the magnetic dynamics sector) can, if necessary, be treated by going beyond the Born-Oppenheimer approximation.

C. Percolation-hopping scenario of transport phenomena in manganites

As discussed in the previous subsection, carrier states in manganites are effectively localized throughout the transition regime. (By effectively localized we mean localized on timescales short compared with that required for the reconfiguration of the magnetic degrees of freedom.) Therefore, in this regime transport of carriers occurs via inelastic hopping (i.e., hopping that is assisted by some inelastic agent such as a phonon). In the following Sec. III C 1, we describe a picture of hopping transport applied to the setting of manganites. Following this, in Sec. III C 2, we use this picture to discuss a scenario for transport phenomena in LCMO and LPMO, which are materials in which polaronic effects are believed to be important. Then, in Sec. III C 3, we describe the scenario of hopping transport suitable for application to LSMO, a material in which signatures of polaronic effects are absent. By contrasting LCMO and LPMO with LSMO we draw some general conclusions concerning the role played by polarons in various manganite compounds.

1. Hopping transport picture in manganites

Hopping transport models based on percolation theory have been successfully applied to transport in systems with states localized by static disorder.[39,42] A peculiarity of manganite systems is that the wavefunctions of states localized in the vicinity of Mn ions depend on the orientations of the Mn core spins on these ions. Inelastic agents (e.g., phonons) lead to hopping between these localized states, the amplitude for such hopping being characterized by matrix elements of the carrier phonon interaction. Therefore, hopping probabilities and rates are determined by the orientations of the core spins. In the double-exchange picture [discussed in more detail in Sec. (III E)], the rate W_{ij} of carrier-hopping between ions i and j, whose core spins (which we treat classically) form an angle θ, is proportional to $\cos^2(\theta/2)$.

As in the standard percolative approach to transport in impurity systems (i.e., the Miller-Abrahams resistive-network approach[42,39,58]), one connects every nearby pair of Mn ions by a bond, and assigns a resistivity to each of these bonds. The charge current J_{ij} between ions i and j is then given by

$$J_{ij}=e(W_{ij}-W_{ij}). \tag{3.1}$$

In the presence of an applied electric field **E** and for a closed external circuit the system out of equilibrium and the charge current is nonzero. If the electric field is sufficiently small [i.e., $e\mathbf{E}\cdot(\mathbf{R}_j-\mathbf{R}_i)\ll kT$], one can expand the charge carrier energies and site occupation numbers to linear order in the electric field. Hence, one can obtain (see e.g., Ref. 39) an expression for the electric current in Ohmic form:

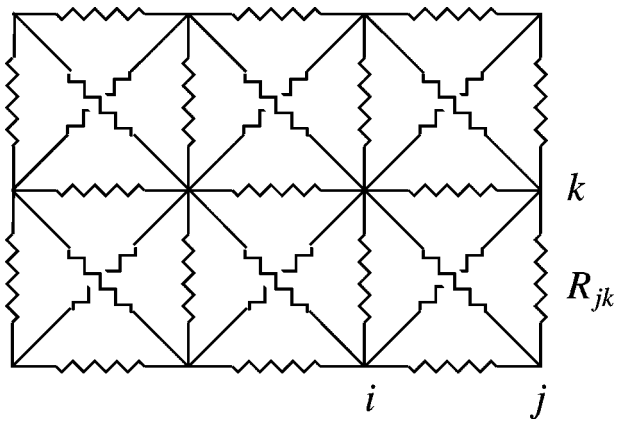

FIG. 9. Schematic picture of the conducting network. Zig-zag line connecting sites i and j represents the resistivity of the bond between these sites.

$$J_{ij}=R_{ij}^{-1}(U_i-U_j), \tag{3.2a}$$

$$R_{ij}=\frac{kT}{e^2W_{ij}^0}, \tag{3.2b}$$

where U_i-U_j is the potential difference between sites i and j in the presence of the electric field, and W_{ij}^0 is the $(\mathbf{E}=\mathbf{0})$ transition rate. Therefore, the resistance R_{ij} of the bond between ions i and j (cf. Fig. 9) is proportional to $1/W_{ij}$, where we have, for the sake of brevity, omitted the superscript 0 (which indicates zero electric fields quantities). The resistances of the bonds constitute a resistive network on which carriers move by taking the least resistive paths, i.e., the transport is percolative in character. The conductivity of the sample is entirely determined by a set of hopping resistivities R_{ij}.

2. Scenario of transport properties in manganites

In the hopping regime, the following scenario for transport properties of manganites can be envisioned.

(i) In the paramagnetic insulating state, i.e., in region I on Fig. 10, the percolative inelastic motion of strongly localized carriers is suppressed by magnetic randomness, via the DE interaction. Although there may exist small clusters of magnetic ions with spins aligned in some direction, neighboring spins (or the spins of neighboring aligned small clusters) are weakly correlated, and are therefore predominantly have a large angle between them. Thus, the resistance of the corresponding resistive bonds is generally large. Hence, the clusters are isolated from each other (i.e., no percolative path exists for which core spins on neighboring Mn ions are approximately aligned), so that outer-shell carriers cannot hop along any path of bonds without encountering a large resistance. Furthermore, if the localization length is on the order

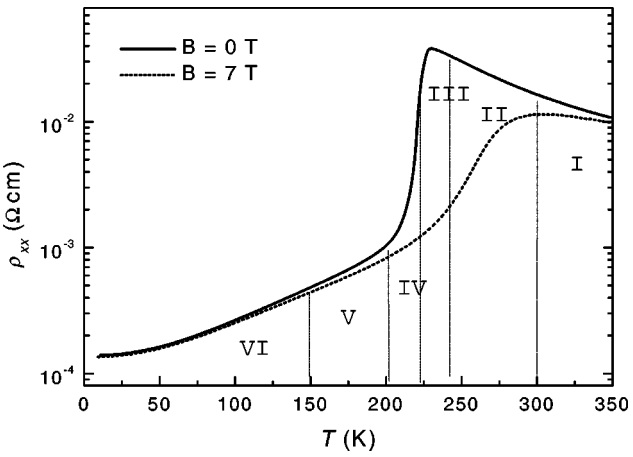

FIG. 10. Transport regimes in manganites exemplified by LCMO. I: High-temperature regime, in which transport is via polarons. II: Crossover to inelastic hopping of charge carriers between localized states. III: Maximal resistivity. In this regime the loss of inelastic agents is compensated by the growth of magnetic order and, hence, the emergence of a conducting network (see text for details). IV: Rapid growth of the conducting network. V: Saturation of the conducting network. VI: Crossover to the metallic regime.

of the lattice constant then carrier interactions with the lattice and carrier self-trapping via small-polaron formation become important. (Below, we shall discuss the situation in which the localization length is larger than the lattice constant.) Carrier self-trapping, when it occurs, does so on very weak (i.e. very resistive) bonds in the resistive network. Deep in the insulating regime, all paths of bonds encounter regions in which carriers are self-trapped. Under these conditions, transport occurs via the rather infrequent hopping of small polarons, which leads to the thermally-activated temperature-dependence of the longitudinal resistivity and Hall coefficient. In the LCMO and LPCMO compounds, the role of polarons in transport accounts for the magnitude of the activation energy associated with the resistivity, which is above 100 meV, and is significantly larger than (any fraction of) the hopping amplitude t.

(ii) With decreasing temperature, the inelastic hopping becomes less frequent, so that the resistivity grows. However, at these temperatures, percolative paths appear that do not encounter regions with self-trapped carriers. Also, the core spins become more aligned with one another, and fairly large clusters exist (that do not feature large resistances connecting pairs of Mn ions having anti-aligned spins). This regime occurs in the range II of temperatures in Fig. 10.

(iii) With continued decrease in temperature, the resistivity reaches a maximum (region III in Fig. 10) when the core spin orientations become sufficiently correlated that a tenuous but infinite conducting network emerges. Due to the still-strong magnetic disorder, as well as any nonmagnetic disorder, the carrier states are still localized (and lie in the band tail). The localization length is on the order of one to two Mn sublattice units. (It is important to note that clusters of spins of size two sublattice units contain some 20 to 30 spins. The alignment of these spins can be obtained by applying magnetic fields of order only a few tesla, leading to colossal magnetoresistance.)

(iv) With yet further reduction in temperature, the resistivity decreases abruptly, in line with the standard percolation picture,[39,42] as more and more inelastic hopping-paths become available to carriers, owing to the increased alignment of core spins (region IV in Fig. 10). The small polarons disappear and, in addition, some of what used to be localized states become delocalized, so that some carriers now populate the states lying on the mobile (i.e., metallic conduction) side of the mobility threshold. (v) The abrupt decrease in resistivity with temperature slows down as soon as any newly available hopping paths are effectively shunted by the existing conducting network (region V in Fig. 10).

(vi) Further decrease in temperature leads to further core-spin alignment and, ultimately, to a significant density of carriers populating states in the conducting part of the band and, hence, to the occurrence of the metallic state (region VI in Fig. 10).

3. Scenario of transport properties of manganites: Absence and presence of polarons

As described in Sec. II B, the temperature dependence of the resistivity does not have a universal form across all manganite compounds. In particular, in LCMO and LPMO, the high-temperature ρ_{xx} is thermally activated, but in LSMO it is not. It is our opinion that the scenario described in points (i)–(vi) in the previous paragraph, which involves self-trapping effects due to polaron formation, takes place in LCMO and LPMO but not in LSMO. This opinion is supported not only by our transport data but also by direct neutron-scattering evidence for the coexistence of distorted and undistorted Mn-O octahedra in the vicinity of T_C,[59–61] as well as by the occurrence of a substantial isotope effect in the resistivity, T_C and thermal expansion.[62]

By contrast, LSMO shows no evidence of polarons in this suite of experiments. Therefore we propose that in LSMO it is only magnetic and static disorder that drive the transition between low- and high-resistance states. According to the scenario described in the previous paragraph, any tendency for the formation of polarons is suppressed when the localization length at the resistive transition (i.e., the inflection point in LSMO) turns out to be larger than a few lattice constants. Because of this, with further increase in the temperature the localization length still has room to decrease due to the suppression of ferromagnetic correlations. This would lead to an increase of the resistivity at temperatures in the immediate vicinity above the resistive transition. Such a resistivity increase has been observed in LSMO.

The significance of polarons in LCMO and LPMO, and their apparent insignificance in LSMO, is consistent with the tendency for polaronic self-trapping to be enhanced for reduced A-site ionic radius, as is the case in the sequence Sr $\rightarrow$Pb$\rightarrow$Ca encountered in our experimental data. The significance of polarons in LCMO and LPMO can also explain why the magnetoresistance of these compounds is stronger than that of LSMO: In LCMO and LPMO, the application of a magnetic field not only results in the tendency to delocalize charge carriers by reducing the magnetic disorder, as it does

in LSMO, but also such magnetic fields destabilize the polaronic regions, leading to a more abrupt reconnection of the network. Furthermore, the presence of polaronic and nonpolaronic spatial regions in LCMO and LPMO enhances disconnection between different parts of the resistive network, and, due to the DE origin of ferromagnetism in these systems, reduces the transition temperature. This ''boot-strap'' collapsing of magnetic order explains why the bare double-exchange energy that determined the spin-wave dispersion at low temperatures is the same for all manganites,[63] even though $T_C^{LCMO}=220$ K, $T_C^{LPMO}=285$ K, and $T_C^{LSMO}=360$ K. We propose that the different sizes of the A-site ions which, in particular, leads to differing-strengths in the static disorder and differing tendencies for self-trapping, is responsible for this trend in the transition temperatures. We also note that the existence of polaronic and nonpolaronic spatial regions in LCMO and LPMO explains the success of the effective medium approaches in predicting the thermoelectric power from the resistivity,[64,65] the observation of both diffusive and continuum electronic signals in Raman scattering,[66] and the presence of significant telegraph noise in the resistivity in these compounds[67]. These features are not characteristic for LSMO.

In Secs. III F–III I and IV, we shall look at the scenario that we have just outlined from the vantage point afforded by the Hall effect. As, in our opinion, the dominant transport mechanism in the transition regime occurs via inelastic hopping between localized states, regardless of whether self-trapping via the formation of small polarons occurs, in Sec. III D we shall first review the basic physical picture underlying the ordinary Hall effect in the inelastic hopping regime in systems having potential (but not magnetic) disorder. The main issues of this discussion are interference of hopping amplitudes in the inelastic hopping regime and elucidation of contribution to the Hall effect in this regime by using properties of the hopping probability with respect to time-reversal symmetry Secs. III D 2–III D 4. (We obtain expressions for hopping amplitudes which differ from those of Holstein in Ref. 23, but this difference is not significant.) Readers familiar with these issues and Holstein theory of the Hall effect can proceed to subsections following this discussion, in which we shall provide an extended discussion of our picture of the microscopic mechanism of the anomalous Hall effect in the hopping regime in manganites, which we have recently proposed.[10,11]

D. Holstein theory of the Hall effect in the hopping regime

Nearly forty years ago, Holstein[23] observed that to capture the ordinary Hall effect in hopping conductors requires the analysis of *at least triads* of sites (i.e., atoms, ions, impurities, etc.), and of the attendant Aharonov-Bohm (AB) magnetic fluxes through the polygons whose vertices are these sites. What Holstein showed was that the probability of the hopping of a charge carrier that is initially located on one of three sites i to one or the other of the remaining sites j (which are initially assumed to be unoccupied), W_{ij} contains a contribution δW_{ij}^{H} that is linear in the applied magnetic field. This dependence arises from interference between the amplitude for a direct (inelastic) transition between the initial and final sites and the amplitude for an indirect (inelastic) transition, involving the intermediate occupation of the third site k. Furthermore, when one applies a magnetic field creating a nonzero magnetic flux through the triangle, thus introducing an Aharonov-Bohm phase for paths that wind around the triangle, the necessity that W_{ij} and W_{ji} be equal is lost, even if $\mathbf{E}\perp(\mathbf{R}_i-\mathbf{R}_j)$. The Hall current, flowing through the bond between sites i and j in a triad of sites, in the presence of such electric field, and in magnetic field perpendicular to the plane containing sites i, j and k, as sketched in Fig. 11, is given by [cf. Eq. (3.1)]

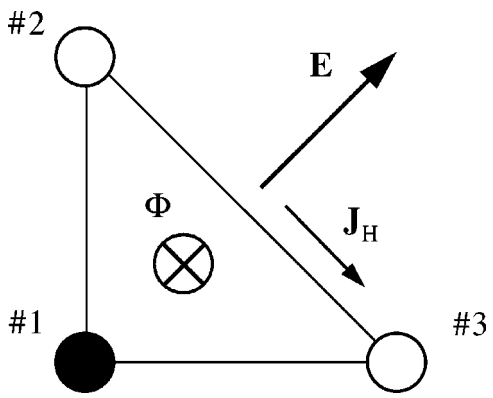

FIG. 11. A triad of sites is the minimal element of the conducting network that leads to a Hall electromotive force. Owing to the flux Φ the carrier current $\mathbf{J}_H$ flows perpendicular to the electric field $\mathbf{E}$. The shaded site is occupied; the unshaded sites are unoccupied.

$$J_{ij}^{H}=e(\delta W_{ij}^{H}-\delta W_{ji}^{H}). \tag{3.3}$$

Such current would cause an increasing imbalance of populations of sites i and j. However, the balance is restored because charge imbalance establishes a chemical potential difference $\Delta\mu_{ij}$ between sites j and i which manifests itself as a Hall voltage. Below in Secs. III F–III I we shall generalize this idea to charge carrier motion in the presence of core spins having inhomogeneous orientations.

1. Ordinary Hall effect: Direct and indirect hopping

Let us now address the issue of the Hall effect at an elementary level. To do this we consider a system of localized carriers, their wave functions $\langle\mathbf{r}|\Psi_j\rangle$ ($j=1,2,\ldots$) being the exact wave functions of the discrete spectrum of the electronic Hamiltonian H_{el} in the presence of ionic potentials, potential disorder and magnetic field. (In order to be specific, we assume, in the present subsection, that the carriers are electrons.)

Now consider the rates of hopping between these exact electronic states caused by the electron-phonon interaction $W_{j\to k}$. The necessity of the electron-phonon interaction (or interactions with some other inelastic agent) for inducing electron hopping will be discussed below in the present subsection. Within the context of hopping rates it is valuable to introduce the notion of *direct* and *indirect* hopping rates. The direct hopping rate $W_{j\to k}^{dir}$ is, to leading order in the electron-phonon interaction, determined by the single direct transition

amplitude, i.e., the electron-phonon interaction matrix element

$$U_{jk}=\langle\Psi_j|H_{\text{el-ph}}|\Psi_k\rangle, \tag{3.4}$$

where $H_{\text{el-}ph}$ is the Hamiltonian of electron-phonon interaction. In Fermi's golden rule approximation $W^{\text{dir}}_{j\to k}$ reads

$$W^{\text{dir}}_{j\to k}=\frac{2\pi}{\hbar}|U_{jk}|^2\delta(E_j-E_k-\hbar\omega), \tag{3.5}$$

where $\{E_i\}$ are the exact energy eigenvalues of H_{el}, and ω is a phonon frequency. There are additive corrections to the direct transition amplitude, which are associated with processes involving phonon-induced scatterings that do not change the electronic state. In addition to the direct transition amplitude, there are amplitudes for indirect transitions from site j to site k, which are defined to be those amplitudes that involve at least one intermediate eigenstate $|\Psi_i\rangle$ (but now i is restricted to be neither j nor k). Among these, there is a subset of amplitudes involving exactly one intermediate eigenstate. Such amplitudes have the following characteristic property: The indirect amplitude that proceeds via a third site i necessarily involves two electron-phonon interaction matrix elements U_{ij} and U_{ki}. Direct and indirect transition amplitudes can interfere, and, as we shall describe below, lead to the Hall effect.

2. Hopping transport: Compatibility of inelastic processes and quantum interference

Despite the apparent simplicity of the foregoing analysis of a triad of sites, the task of obtaining the linear dependence of the Hall resistivity on the magnetic field via Holstein's approach is a much more subtle matter. Furthermore, the issue of establishing quantal interference effects in this setting of inelastic hopping processes is equally subtle, so we shall now revisit this subject.

Why is it that we need to consider inelastic processes when considering the Hall effect? As for the longitudinal hopping conductivity of localized carriers, it is due to electronic quantum transitions between localized carrier eigenstates, assisted by phonons (or some other inelastic agent). The participation of some inelastic agent in hopping conduction is required for the following reasons. First, owing to carrier localization, the conductivity of the carrier system in the absence of phonons is that of an Anderson insulator, i.e., zero. Phonons cause transitions between localized carrier states and, hence, allow conduction. Second, phonon-assisted carrier transitions meet the need to have carrier transitions between occupied states (which lie below the Fermi level) and unoccupied states (which lie above the Fermi level) whilst satisfying the demand that energy be conserved (Fig. 12). This energy-conservation requirement also holds for the Hall effect. Now, as inelastic processes are being invoked one should ask the question: How can interference between distinct hopping paths, necessary for the sensitivity of the hopping rate to any quantal phase, arise?

We will answer this question both in the context of longitudinal conductivity and the Hall effect. In the next subsubsection we will consider the longitudinal conductivity.

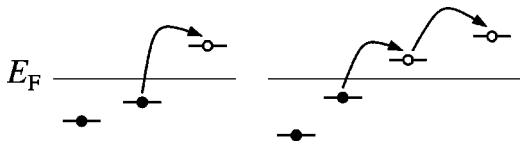

FIG. 12. Schematic depiction of phonon-assisted inelastic hopping. Direct hopping (left) and indirect coherent hopping via an intermediate site (right) are shown.

After that, in further sections, we will discuss what inelastic processes contribute to the Hall effect, and interference of those processes.

3. Quantum interference in the presence of inelastic scattering. Longitudinal conductivity

In order to answer the question posed in the previous section let us first formulate precisely what is meant by coherence and sensitivity to the quantal phase in the system at hand. The Hamiltonian of the system reads

$$H=H_{\text{el}}+H_{\text{el-ph}}+H_{\text{ph}}, \tag{3.6}$$

where H_{ph} is the phonon Hamiltonian. The exact quantum-mechanical eigenstates of H_{el}, both localized and delocalized, are sensitive to applied magnetic field. (Here, we are, of course, concerned with localized states.) In the presence of a magnetic field, the exact eigenfunctions $\langle\mathbf{r}|\Psi_j\rangle$ can no longer be chosen to be real quantities, and are thus characterized by an absolute value and a phase. It is often convenient to approximate the exact localized eigenstates in terms of the eigenstates $\{|\phi_j\rangle\}$ of outer-shell electrons of isolated ions (where i enumerates the ions). We note that the $\{|\phi_j\rangle\}$ are not, in general, orthogonal, although they are typically linearly independent and may, therefore, be taken as a basis. In terms of this basis a Hamiltonian describing carrier motion in the presence of the corresponding isolated ions located at positions $\{\mathbf{R}_j\}$ as well as a disordered potential has the form

$$H_{\text{el}}=\sum_j|\phi_j\rangle\epsilon_j\langle\phi_j|+\sum_{j\neq k}|\phi_j\rangle V_{jk}\langle\phi_k|, \tag{3.7}$$

where $\{\epsilon_j\}$ are random energies and V_{jk} are random transfer matrix elements.

Having introduced the basis of localized ionic states $\{|\phi_j\rangle\}$ and the Hamiltonian for the disordered system of ions H_{el}, we now examine in detail the effect on this system of an applied magnetic field. As shown by Holstein,[23] in the presence of a magnetic field the ionic basis states $\{|\phi_j\rangle\}$ become the modified collection $\{|\phi_j\rangle_B\}$, being solutions of the Schrödinger equation

$$\left[\frac{1}{2m^*}\left(\mathbf{p}+\frac{e\mathbf{A}}{c}\right)^2-U(\mathbf{r}-\mathbf{R}_j)\right]\langle\mathbf{r}|\phi_j\rangle_B=\epsilon\langle\mathbf{r}|\phi_j\rangle_B, \tag{3.8}$$

where $U(\mathbf{r}-\mathbf{R}_j)$ is the potential of the ion located at position $\mathbf{R}_j$, m^* is the effective mass, and $\mathbf{A}$ is the magnetic vector potential. The wave function $\langle\mathbf{r}|\phi_j\rangle_B|_{B=0}$ has the property that it is a function of $\mathbf{r}-\mathbf{R}_j$, and we would like to recover

something like this property in the presence of the magnetic field. To do this we introduce a gauge transformation

$$\langle \mathbf{r}|\phi_j\rangle = \langle \mathbf{r}|\kappa_j\rangle e^{-i\eta_j(\mathbf{r})}, \tag{3.9a}$$

$$\eta_j(\mathbf{r}) = (e/\hbar c)\mathbf{A}(\mathbf{R}_j)\cdot\mathbf{r} = (e/\hbar c)(\mathbf{B}\times\mathbf{R}_j)\cdot\mathbf{r}, \tag{3.9b}$$

where we have chosen the gauge potential to be $\mathbf{A}(\mathbf{r})=\mathbf{H}\times\mathbf{r}/2$. It is straightforward to show that this transformation leads to an equation for $\langle \mathbf{r}|\kappa_j\rangle$ in which the vector potential (magnetic field) term contains a coordinate in combination $(\mathbf{r}-\mathbf{R}_j)$:

$$\left[\frac{1}{2m^*}[\mathbf{p}+e\mathbf{H}\times(\mathbf{r}-\mathbf{R}_j)/2c]^2 - U(\mathbf{r}-\mathbf{R}_j)\right]\langle \mathbf{r}|\phi_j\rangle_B = \epsilon\langle \mathbf{r}|\phi_j\rangle_B . \tag{3.10}$$

Hence, the wave function $\langle \mathbf{r}|\kappa_j\rangle$ is seen to have the sought property

$$\langle \mathbf{r}|\kappa_j\rangle_B = \langle \mathbf{r}-\mathbf{R}_j|\kappa_j\rangle. \tag{3.11}$$

It is convenient to employ the magnetic-field dependent ionic states $\{|\phi_i\rangle_B\}$ in the perturbative construction of the eigenstates of the system Hamiltonian (3.7)

$$H_{\rm el}(\mathbf{B}) = \sum |\phi_j\rangle_B \epsilon_j(\mathbf{B})\langle\phi_j|_B + \sum_{j\neq k} |\phi_j\rangle_B V_{jk}(\mathbf{B})\langle\phi_k|_B . \tag{3.12}$$

In what follows we shall omit the explicit dependence on **B**.

We now construct approximations to the exact eigenstates of $H_{\rm el}(\mathbf{B})$ in terms of linear combinations of ionic states $\{|\phi_i\rangle_B\}$. To do this we use renormalized (i.e., Brillouin-Wigner) perturbation theory in powers of $V_{kj}/(E_j-E_k)$ (see, e.g., Refs. 68 and 69), thus obtaining

$$|\Psi_j\rangle = |\phi_j\rangle + \sum k(\neq j)|\phi_k\rangle \times\left[\frac{V_{kj}}{E_j-E_k} + \sum_{\substack{k(\neq j)\\ h(\neq j)}} \frac{V_{kh}V_{hj}}{(E_j-E_k)(E_j-E_h)} + \cdots\right], \tag{3.13}$$

where $\{E_j\}$ are the exact energy eigenvalues. We now pause to remark that in the theory of hopping conductivity in doped semiconductors[58,39,42,23] the parameter $V_{kj}/(E_j-E_k)$ is indeed small, due to sizable distance between donors (or acceptors). In subsection devoted to application of hopping conductivity model to manganites we will see that this parameter can also be rendered as small, because of the dependence of the effective hopping amplitude on the core-spin misalignment. It is worth mentioning, however, that the sensitivity of $|\Psi_j\rangle$ to phases arising from transformation Eq. (3.9a) is a general property which does not rely on perturbation expansion (3.13). It is also reasonable to assert that the essential dependence of $\{|\Psi\rangle_j\}$ on the magnetic field enters solely through such phase acquired by the local basis wave functions $\{\langle \mathbf{r}|\phi_j\rangle\}$ under the gauge transformation in Eq. (3.9a), because, at reasonable experimental strengths of the magnetic field much less than a quantum of flux treads a localized ionic wave function.

Having constructed the states $|\Psi_j\rangle$, i.e., approximations to the exact localized states, we now use them to compute the square modulus of the matrix element U_{jk} of Eq. (3.4):

$$\begin{aligned}|U_{jk}|^2 &= |\langle\Psi_j|H_{\text{el-ph}}|\Psi_k\rangle|^2 \\ &= \cdots + \sum_{i\neq k}\sum_{n\neq k, n\neq i} \langle\phi_k|H_{\text{el-ph}}\phi_j|\phi_j\rangle\langle\phi_j|H_{\text{el-ph}}|\phi_k\rangle \\ &\times \frac{V_{ik}V_{kn}V_{ni}}{(E_i-E_k)^2(E_i-E_n)} \\ &+ \sum_{m\neq j}\sum_{l\neq m, l\neq j} \langle\phi_i|H_{\text{el-ph}}|\phi_m\rangle \\ &\times \langle\phi_m|H_{\text{el-ph}}|\phi_i\rangle \frac{V_{mj}V_{jl}V_{lm}}{(E_j-E_m)^2(E_j-E_l)} + \text{c.c.} + \cdots,\end{aligned} \tag{3.14}$$

which features in the transition rate, Eq. (3.5).

Terms exhibited in Eq. (3.14) involve motion along paths that surround loops of nonzero area, i.e., the matrix elements of electron-phonon interaction and transfer amplitudes are taken between localized orbitals Eq. (3.8) of sites that form such loops. Note, however, that not all such terms are included in Eq. (3.14), but only those in which matrix elements of electron-phonon interaction enter the corresponding expressions in combination with their complex conjugated (i.e., time-reversed) counterparts. Furthermore, the remaining matrix elements entering terms featured in Eq. (3.14), i.e., the overlap integrals V_{hk}, involve motion along paths that surround loops of nonzero area.[70] It is through such products of three overlap integrals $V_{hk}V_{kj}V_{jh}$ that the transition rate acquires its sensitivity to fluxes through loops of nonzero area. It is only such terms that lead to nonvanishing interference contribution to hopping probability which is sensitive to fluxes. Such sensitivity to phase results in the Aharonov-Bohm magnetoresistance effects in hopping conductivity (see, e.g., Ref. 71).

Let us discuss the physical meaning of interference terms featured in Eq. (3.14). Consider, for example, charge carrier hopping in a triad of sites. The relevant terms in Eq. (3.14), which involve loops, correspond to $i=1$, $j=2$, $k=2$, $n=3$ (in the first of featured terms), and $m=1$, $l=3$ (in the second of featured terms). In terms of isolated orbitals the first term features in Eq. (3.14) corresponds to interference of two processes of charge carrier tunneling from site 1 to site 2, a direct one and an indirect one (via site 3), with the following charge carrier interaction with a phonon at site 2; the second term corresponds to carrier interaction with phonon at site 1 with the following interference between direct and indirect tunneling paths from site 1 to site 2. (We note that the situation can, of course, be readily generalized to the case of changes in more than one phonon occupation number.)

We now notice that by contrast with terms that are featured in Eq. (3.14), terms that have been omitted there, like

$$\delta|U_{jk}|^2=\sum_{k\neq i}\langle\phi_i|H_{\text{el-ph}}|\phi_j\rangle\langle\phi_j|H_{\text{el-ph}}|\phi_k\rangle\frac{V_{ki}}{E_i-E_k}, \tag{3.15}$$

involve motion along paths that surround loops of nonzero area, but do not lead to nonvanishing interference contribution to hopping probability. The reason for absence of such contributions is that they do not involve combinations of matrix elements of electron-phonon interaction with their time-reversed counterparts. To see why such combinations are important, consider the electron-phonon interaction Hamiltonian

$$H_{\text{el-ph}}=\sum_{\mathbf{q}} H_q e^{i\mathbf{q}\cdot\mathbf{r}}, \tag{3.16}$$

where **q** is the phonon wave vector. Evaluation of nonvanishing interference contribution, therefore, includes sums over all phonon wave vectors. Terms that exhibit two matrix elements of electron-phonon interaction that are not complex conjugated to each other turn out to be oscillating functions of **q**, and vanish upon evaluation of the sum over **q**. This simple observation allows us to find all important interference terms in the hopping probability (3.14) without resorting to explicit evaluation of $\langle\phi_i|H_{\text{el-ph}}|\phi_j\rangle$ as it was done, e.g., in Ref. 23 in consideration of the Hall effect and in Ref. 69 in consideration of the Aharonov-Bohn hopping magnetoresistance. We note that if the sum of two terms featured in Eq. (3.14) is equal to zero, this consideration easily allows us to find the appropriate next terms of expansion of hopping probability in powers of $V_{ij}/(E_i-E_j)$.

We are now in a position to discuss what is meant by phase coherence and sensitivity to quantal phases in the present setting of hopping conduction. In the absence of inelastic agents, products of, e.g., three overlap integrals $V_{hk}V_{kj}V_{jh}$ (where sites *h*, *k* and *j* form a nondegenerate triangle, with nonzero flux threading this triangle in the presence of magnetic field), and carrier energies E_j (see the remark[70]) are sensitive to the Aharonov-Bohm quantal phase. As we can see from Eq. (3.14), interference of two amplitudes of quantal transition between states *h* and *k* occurs (and these amplitudes are coherent) even if these transitions are due to inelastic agents. For such interference to occur, inelastic agents which determine one of the amplitudes of the transition must be the same as inelastic agents which determine another amplitude of the transition (i.e., phonon frequencies and wave vectors are equal), so that the square modulus of matrix element of, e.g., the electron-phonon interaction, enters the probability. As we have mentioned above, the presence of square modulus of the electron-phonon interaction matrix element in the probability corresponds to phonon factors in the two interfering amplitudes (e.g., in the amplitude of a direct process and in the complex conjugate of the amplitude of an indirect process) being related to each other by the time reversal.

Let us now discuss what is meant by the phase breaking or decoherence in the context of the hopping conductivity regime. The eigenstates $\{|\Psi\rangle_j\}$ and their energies E_j are determined by $H_{\text{el-ph}}$, i.e., in the absence of phonons. When phonons interact with charge carriers, one can consider them as a reservoir which leads to randomization of carrier states. The time scale of such randomization is given by the inverse rate of carrier transitions between different eigenstates of $H_{\text{el-ph}}$ caused by electron-phonon interaction (3.5). It is this randomization that is meant by phase breaking (or decoherence). However, the carrier transition rate (3.5) between different states itself, which measures the rate of decoherence (being determined by eigenfunctions of these states) carries information about quantal phases that arise in the context of Eqs. (3.13) and (3.14). Furthermore, the electric current arises during the act of hopping, i.e., when randomization has not yet occurred. Therefore, the answer to the question, posed in the second paragraph of the present subsection, concerning interference in the presence of inelastically-assisted hopping is as follows: The (steady-state) hopping current is generated during the process of inelastic scattering, whilst decoherence arises only after this scattering has occurred; thus, decoherence effects do not preclude sensitivity of hopping conduction to quantal phases. Moreover, the question of interference of consequent hopping events is meaningless in the context of hopping conductivity, because only amplitudes of hopping between the same initial and the same final states can interfere. Thus, there is a significant difference between interference effects in hopping conductivity and in diffusive mesoscopic transport. In diffusive transport, the whole diffusive trajectory, with all consequent scattering events, determines the current via the diffusivity, and electronic coherence during consequent scattering events is important for interference effects. In hopping transport, incoherence of consequent hopping events does not contradict interference of quantum-mechanical amplitudes that determine a single charge carrier hop and the hopping current itself.

4. Quantum interference in the presence of inelastic scattering; processes leading to the Hall effect

For localized carriers, the interference processes that lead to the Hall conductivity are even more peculiar than those leading to the sensitivity of the longitudinal conductivity to the Aharonov-Bohm phase. In particular, the occurrence of the Hall effect requires phonon-assisted hoppings between exact initial and final carrier states, via an exact intermediate state. [It is not sufficient to include as intermediate states the virtual ionic orbitals that enter via Eq. (3.13).] The reason for this difference between the hopping Hall conductance and the sensitivity to magnetic flux of the hopping magnetoconductance arises because of the necessity to extract a dependence of the Hall conductance that is *linear* in (or, more generally, an odd power of) the magnetic field .

Let us now explore the collection of processes that contribute to the Hall conductance. These processes, first identified by Holstein, can be determined by making use of the odd (i.e., dissipative) character of transition rates under the time-reversal operation: $t\rightarrow -t$. As discussed in Secs. III C and III D, the hopping current is determined, via the conductivities of the resistive network, by the rate of transitions between sites. The Hall current, as with any current, is odd under time reversal. So, too, is the transition rate. (To appre-

ciate this, consider an elementary relaxation process for some quantity Q, which evolves according to the rate equation

$$\frac{dQ}{dt} \equiv -\frac{Q}{\tau}. \tag{3.17}$$

From the consistency of equation one immediately sees that it is formally appropriate to designate the relaxation rate τ as being odd under the time reversal.) Now consider the transition probability per unit time between the exact single-carrier states i and f, viz. W_{fi} which, according to Fermi's golden rule, is given by

$$W_{fi} = \frac{2\pi}{\hbar} |A_{fi}|^2 \delta(E_i - E_f), \tag{3.18}$$

where A_{fi} is the sum of the transition amplitudes for all coherent (i.e., interfering) processes connecting i and f, and the δ function imposes energy conservation between the initial and final states, the energies E_i and E_f of these states being full energies. (That is, they include not only carrier but also phonon energies.) The δ-function, which has the complex representation

$$\delta(E) = \mathrm{Im} \frac{1}{\pi} \lim_{s \to +0} \frac{i}{E - is}, \tag{3.19}$$

is an odd quantity with regard to time-reversal, in the sense that under the transformation $t \to -t$, sign of imaginary part s in the denominator changes and, thus, so does the sign of the δ function. By contrast, the quantity $|A_{fi}|^2$ is even (i.e., nondissipative) under time reversal. We note, in passing, that the precision of the energy conservation is not what is essential (from the point of view of time-reversal properties). For example, the imaginary part of a Lorentzian function,

$$\mathrm{Im} \frac{1}{\pi} \frac{i}{E - i\Gamma} = \frac{1}{\pi} \frac{\Gamma}{E^2 + \Gamma^2}, \tag{3.20}$$

reveals that this function, too, inherits the oddness of the rate Γ.

En route to exploring the processes that contribute to the Hall conductance, let us now consider a simple case in which A_{fi} has just two contributions:

$$A_{fi} = A_{fi}^{\mathrm{dir}} + A_{fi}^{\mathrm{ind}}, \tag{3.21}$$

where A_{fi}^{dir} is the amplitude for the direct path and A_{fi}^{ind} is the amplitude for an indirect path (i.e., a path via an intermediate state). These two amplitudes can be written in the form

$$A_{fi}^{\mathrm{dir}} = A_{fi}^{0,\mathrm{dir}} \exp i\phi_1, \tag{3.22a}$$

$$A_{fi}^{\mathrm{ind}} = A_{fi}^{0,\mathrm{ind}} \exp i\phi_2, \tag{3.22b}$$

$$\phi = \phi_1 - \phi_2, \tag{3.22c}$$

where $A_{fi}^{0,\mathrm{dir}}$ and $A_{fi}^{0,\mathrm{dir}}$ are the zero-magnetic-field amplitudes, and ϕ_1 and ϕ_2 are phases arising in the presence of magnetic field for direct and indirect paths, correspondingly, and ϕ is

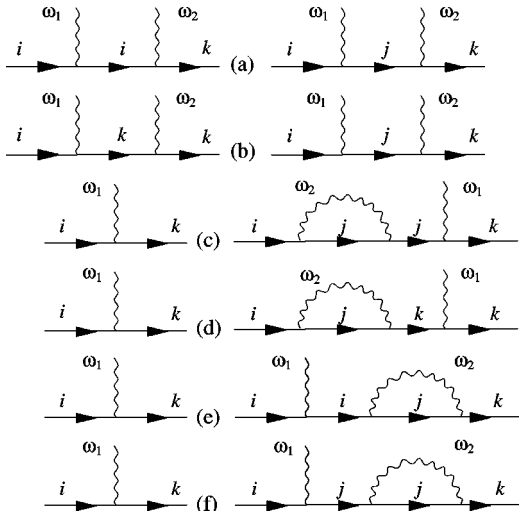

FIG. 13. Pairs of interfering amplitudes that result in the Hall effect. Rows (a) and (b) each show the interference of two-stage processes. Rows (c) to (f) each show the interference of a one-stage and a three-stage process. Right column: indirect hopping processes; left column: direct hopping processes. Lines with arrows correspond to carrier propagators; their intersections with wavy lines correspond to matrix elements of carrier-phonon interactions.

the difference of phases between direct and indirect paths induced by magnetic field, i.e., the Aharonov-Bohm phase. (We neglect changes magnetic-field-induced changes in the magnitudes of $A_{fi}^{0,\mathrm{dir}}$ and $A_{fi}^{0,\mathrm{dir}}$.) For the transition probability we then have

$$|A_{fi}|^2 = |A_{fi}^{0,\mathrm{dir}}|^2 + |A_{fi}^{0,\mathrm{ind}}|^2 + \mathrm{Re}\, A_{fi}^{0,\mathrm{dir}*} A_{fi}^{0,\mathrm{ind}} \cos\phi + \mathrm{Im}\, A_{fi}^{0,\mathrm{dir}*} A_{fi}^{0,\mathrm{ind}} \sin\phi. \tag{3.23}$$

We now observe that the term containing $\sin\phi$ is the only contribution to the probability $|A_{fi}|^2$ that is odd with respect to the transformation $\phi \to -\phi$ (i.e., with respect to magnetic-field reversal), this oddness being a necessary property of the Hall conductance. Thus, in a computation of the Hall conductance, only the imaginary part of the quantity corresponding to $A_{fi}^{0,\mathrm{dir}*} A_{fi}^{0,\mathrm{ind}}$ contributes and, therefore, one has to consider those indirect processes for which the zero-magnetic-field amplitude has a component out-of-phase with the zero-magnetic-field amplitude of the direct process. (Said another way, one must consider contributions to $A_{fi}^{0,\mathrm{dir}*} A_{fi}^{0,\mathrm{ind}}$ that are odd with respect to time reversal.) Such contributions do not appear if, as in the case of the longitudinal hopping conductivity in Sec. III D 3, one considers one-phonon processes.[72] They do, however, appear if one considers, e.g., two-phonon processes described by combinations of amplitudes obeying the following property: $A_{fi}^{0,\mathrm{dir}}$ contains an even (odd) number of complex energy denominators when $A_{fi}^{0,\mathrm{ind}}$ contains an odd (even) number. Then these denominators give rise to an additional energy-conserving δ function,[73] a quantity that is odd respect to time reversal [cf. Eq. (3.19)], and yields contributions to the probability that behave suitably under time reversal.

Having ascertained the structure of the amplitudes that give rise to the Hall effect, we now select and examine the dominant contributing processes (i.e., those involving the smallest possible number of electron-phonon interactions). These involve two-phonon transitions and, as shown by Holstein,[23] their elements (i.e., direct and indirect processes) can be visualized as follows.

(i) Both transitions are two-stage processes (i.e., involve two transitions between exact carrier states). For example, the indirect and indirect transitions respectively being

$$(i,N_1,N_2)\rightarrow(j,N_1',N_2)\rightarrow(k,N_1',N_2'), \tag{3.24a}$$

$$(i,N_1,N_1)\rightarrow(i,N_1',N_2)\rightarrow(k,N_1',N_2'), \tag{3.24b}$$

where N_1, N_1', N_2 and N_2' are the occupation numbers of phonon modes 1 and 2, N, and N' differ by unity, i, j, and k label initial, intermediate and final sites (as well as carrier states localized on these sites).

(ii) The direct transition is a one-stage process, e.g.,

$$(i,N_1)\rightarrow(k,N_1'), \tag{3.25a}$$

and the indirect transition is a three-stage process, e.g.,

$$(i,N_1,N_2)\rightarrow(i,N_1',N_2)\rightarrow(j,N_1',N_2')\rightarrow(k,N_1',N_2). \tag{3.25b}$$

(The whole set of processes includes those which result from alterations of the sequences of various subprocesses.) One can observe, that phonon modes whose population is changed in processes (i) or (ii), interact with charge carrier on both direct and indirect path, and, as we shall see, these paths can interfere.[74] Complete set of processes that lead to the Hall effect is shown on Fig. 13.

In terms of phonon-assisted transitions between exact carrier eigenstates $|\Psi_i\rangle$, the two-stage processes are described by the amplitudes

$$A^{\mathrm{dir},2}_{k,N_1,N_2;j,N_1',N_2'}=\frac{\langle\Psi_k,N_1|H_{\text{el-ph}}|\Psi_k,N_1'\rangle\langle\Psi_k,N_2|H_{\text{el-ph}}|\Psi_i,N_2'\rangle-\langle\Psi_k,N_2|H_{\text{el-ph}}|\Psi_i,N_2'\rangle\langle\Psi_i,N_1|H_{\text{el-ph}}|\Psi_i,N_1'\rangle}{E_j-E_k}$$
$$+\frac{\langle\Psi_k,N_2|H_{\text{el-ph}}|\Psi_k,N_2'\rangle\langle\Psi_k,N_1|H_{\text{el-ph}}|\Psi_i,N_1'\rangle-\langle\Psi_k,N_1|H_{\text{el-ph}}|\Psi_i,N_1'\rangle\langle\Psi_i,N_2|H_{\text{el-ph}}|\Psi_i,N_2'\rangle}{E_i-E_j}, \tag{3.26a}$$

$$A^{\mathrm{ind},2}_{k,N_1,N_2;j,N_1',N_2'}=\frac{\langle\Psi_k,N_1|H_{\text{el-ph}}|\Psi_j,N_1'\rangle\langle\Psi_j,N_2|H_{\text{el-ph}}|\Psi_i,N_2'\rangle}{E_i-E_j+(N_1'-N_1)\hbar\omega_1+i\hbar\gamma}+\frac{\langle\Psi_k,N_2|H_{\text{el-ph}}|\Psi_j,N_2'\rangle\langle\Psi_j,N_1|H_{\text{el-ph}}|\Psi_i,N_1'\rangle}{E_i-E_j+(N_2'-N_2)\hbar\omega_2+i\hbar\gamma}, \tag{3.26b}$$

where $A^{\mathrm{dir},2}_{k,N_1,N_2;j,N_1',N_2'}$ and $A^{\mathrm{ind},2}_{k,N_1,N_2;j,N_1',N_2'}$ are, respectively, the amplitudes of the two-stage-direct and two-stage-indirect processes. The interfering amplitudes for the one-stage process $A^{\mathrm{dir},1}$ and (an example of) a three-stage process $A^{\mathrm{ind},3}$ are given in terms of the exact carrier eigenstates $|\Psi_i\rangle$:

$$A^{\mathrm{dir},1}=\langle\Psi_k,N_1|H_{\text{el-ph}}|\Psi_i,N_1'\rangle, \tag{3.27a}$$

$$A^{\mathrm{ind},3}=\frac{\langle\Psi_k,N_2|H_{\text{el-ph}}|\Psi_j,N_2'\rangle\langle\Psi_j,N_2'|H_{\text{el-ph}}|\Psi_j,N_2\rangle\langle\Psi_j,N_1|H_{\text{el-ph}}|\Psi_i,N_1'\rangle}{(E_i-E_j)(E_i-E_j+(N_1'-N_1)\hbar\omega_1+i\hbar\gamma)}. \tag{3.27b}$$

Let us briefly discuss the energy conservation (i.e. δ-function) structure and time-reversal properties of the probabilities associated with the amplitudes given in Eqs. (3.26a), (3.26b), (3.27a), and (3.27b). The explicit δ function in the formula (3.18) for W_{fi} constrains the energies of the initial and final states. One further δ function arises when we insert explicit expressions for the interfering pairs of amplitudes, Eqs. (3.26a), (3.26b) and Eqs. (3.27a), (3.27b), into Eq. (3.18). This second δ function characterizes energy conservation between initial and intermediate (or intermediate and final states). As we mentioned earlier, time reversal symmetry can also be satisfied if we use, e.g., imaginary parts of Lorentzian functions instead of δ functions, thus taking into account approximate energy conservation in transitions between broadened states of the system. Here, for brevity, we use the term δ function when discussing time-reversal properties of transition rates.

Let us follow how these δ functions (and, hence, the requisite odd character under time reversal) emerge. For two-stage processes, a direct transition has to contain one intermediate state, which has to be virtual state, and, therefore Eq. (3.26a) contains real energy denominators. Thus, in two stage processes, a δ function additional to one giving energy conservation between initial and final state, is to arise from indirect transition amplitudes. Such a δ function indeed arises (in each of the contributing terms) from complex denominators of Eq. (3.26b), upon summation over all possible phonon modes. In interference involving three-stage pro-

cesses, the analytical expression for three-stage amplitude Eq. (3.27b) is characterized by two energy denominators. Upon summation over all possible phonon modes, one of these denominators leads to a δ function. Another energy denominator in Eq. (3.27b) corresponds to a virtual transition. As follows from Eq. (3.23), in the presence of the Aharonov-Bohm phase ϕ picked up by carriers moving around three sites, interference contributions to W_{if} determined by Eqs. (3.26a) and (3.26b) and by Eqs. (3.27a) and (3.27b) all contain two δ functions, and, as required by time-reversal symmetry properties, are proportional to $\sin\phi$.

In order to see the physical meaning of interference between amplitudes of direct and indirect two-stage processes or interference between amplitudes of one- and three-stage processes, it is instructive to write down the amplitudes (3.26a), (3.26b), (3.27a), and (3.27b) in terms of the ionic orbitals $|\phi_i\rangle$ and the transfer integrals V_{ij}, by using Eq. (3.13). (The energy denominators are corrected compared to those that can be found in the original Holstein paper[23]). This will also allow us to formulate conditions necessary for coherence of two-phonon processes, relevant for the Hall effect.

In terms of $|\phi_i\rangle$ and V_{ij}, the two-stage processes are described by the amplitudes

$$A^{\mathrm{dir},2}_{k,N_1,N_2;j,N_1',N_2'}=\frac{\langle\phi_k,N_1|H_{\text{el-ph}}|\phi_k,N_1'\rangle\langle\phi_i,N_2|H_{\text{el-ph}}|\phi_i,N_2'\rangle V_{ki}-\langle\phi_k,N_2|H_{\text{el-ph}}|\phi_k,N_2'\rangle\langle\phi_i,N_1|H_{\text{el-ph}}|\phi_i,N_1'\rangle V_{ki}}{(E_j-E_k)(E_i-E_k)}$$
$$+\frac{\langle\phi_k,N_2|H_{\text{el-ph}}|\phi_k,N_2'\rangle\langle\phi_i,N_1|H_{\text{el-ph}}|\phi_i,N_1'\rangle V_{ik}-\langle\phi_k,N_1|H_{\text{el-ph}}|\phi_k,N_1'\rangle\langle\phi_i,N_2|H_{\text{el-ph}}|\phi_i,N_2'\rangle V_{ik}}{(E_i-E_j)(E_k-E_i)} \tag{3.28a}$$

$$A^{\mathrm{ind},2}_{k,N_1,N_2;j,N_1',N_2'}=\frac{\langle\phi_k,N_1|H_{\text{el-ph}}|\phi_k,N_1'\rangle\langle\phi_i,N_2|H_{\text{el-ph}}|\phi_i,N_2'\rangle V_{jk}V_{ij}}{(E_i-E_j+(N_1'-N_1)\hbar\omega_1+i\hbar\gamma)(E_k-E_j)(E_i-E_j)}+\frac{\langle\phi_k,N_2|H_{\text{el-ph}}|\phi_j,N_2'\rangle\langle\phi_j,N_1|H_{\text{el-ph}}|\phi_i,N_1'\rangle}{E_i-E_j+(N_2'-N_2)\hbar\omega_2+i\hbar\gamma}. \tag{3.28b}$$

The interfering amplitudes for the one-stage process $A^{\mathrm{dir},1}$ and an example of a three-stage process $A^{\mathrm{ind},3}$ which, in terms of exact carrier states, are given by Eqs. (3.27a) and (3.27b) in terms of ionic orbitals read

$$A^{\mathrm{dir},1}=\frac{\langle\phi_k,N_1|H_{\text{el-ph}}|\phi_k,N_1'\rangle V_{ki}+\langle\phi_i,N_1|H_{\text{el-ph}}|\phi_i,N_1'\rangle V_{ki}}{E_i-E_k}, \tag{3.29a}$$

$$A^{\mathrm{ind},3}=\ldots+\frac{\langle\phi_j,N_2|H_{\text{el-ph}}|\phi_j,N_2'\rangle\langle\phi_j,N_2'|H_{\text{el-ph}}|\phi_j,N_2\rangle\langle\phi_i,N_1|H_{\text{el-ph}}|\phi_i,N_1'\rangle V_{kj}V_{ji}}{(E_j-E_k)(E_i-E_j)(E_i-E_j+(N_1'-N_1)\hbar\omega_1+i\hbar\gamma)}. \tag{3.29b}$$

First term in Eq. (3.29a) does not contribute to interference of one- and three-stage processes, because the matrix element $\langle\phi_k,N_1|H_{\text{el-ph}}|\phi_k,N_1'\rangle$ does not correspond to any time-reversed counterpart in Eq. (3.29b). We are now in a position to discuss the physical meaning of processes that contribute to the Hall effect in terms of local orbitals. In the interference of two stage processes, both amplitudes, direct and indirect, correspond to interaction with a phonon mode (N_1,ω_1) at site k (initial state $|\phi_k\rangle$, tunneling to site i (final state $|\phi_i\rangle$) directly or via intermediate site j, and interacting with a phonon mode (N_2,ω_2) (at site i) that is distinct from one participating in a process occurring at site k. In the interference of one- and three-stage processes, the direct one-stage process (which is, strictly speaking, can be called one-stage only in terms of exact carrier states) can include two possibilities: (i) Interaction with a phonon mode (N_1,ω_1) at initial site and tunneling to the final site; (ii) tunneling to the final site and interaction with a phonon mode (N_1,ω_1) at the final site. Then the three stage process have to include the following stages: In the case (i) there is interaction with the phonon mode (N_1,ω_1) at initial site, tunneling to intermediate site j, emission (absorption) and reabsorption (reemission) of a phonon mode (N_2,ω_2) at site j, and tunneling to the final site. In the case (ii) charge carrier tunnels to intermediate site j, where emission (absorption) and reabsorption (reemission) of a phonon mode (N_2,ω_2) occurs, and then tunnels to the final site. We therefore see that, in terms of local orbitals, processes contributing to the Hall effect are characterized by interference of amplitudes in which phonon modes changing their occupation numbers are represented by time reversed counterparts in A^{dir} and A^{ind}, respectively.

Having described the inelastic processes leading to the Hall effect, we are now in the position to generalize conditions for occurrence of interference, and to formulate these conditions for two-phonon processes. It follows from Eqs. (3.26b), (3.26a), (3.27a), and (3.27b) that electron-phonon interaction results in coherence of transfer amplitudes in two cases: (i) If direct transition and transition via an intermediate state both occur as two-phonon processes,[72] with two phonon modes changing their occupation numbers in the

course of both these transitions, then interference exists when the two phonons leading to the direct transition are the same as two phonons leading to a transition via intermediate site; (ii) if the direct transition occurs as one-stage process assisted by a phonon mode, this phonon mode changes its occupation number, and the transition involving an intermediate site occurs as a three stage process. Then, the condition is that one of the phonon modes assisting three-stage process is the same as that in the direct transition, while another phonon mode which assists the indirect transition does not change its occupation number.

Broadly speaking, both these cases lead to conditions that inelastic modes that change their state in the course of electronic hop are the same in the two interfering hopping amplitudes. Only in this case an interference exists even between amplitudes of inelastic processes. We note that this point has been also recently revisited by Entin-Wohlman *et al.*[76]

5. Ordinary Hall effect: Local conductivities. Remarks on averaging over triads

These interference contributions will result in the ordinary Hall effect, with the Hall conductivity in a triad of ions $\sigma_{\rm OH}$ given by

$$\sigma_{\rm OH}=G\{\epsilon_j\}\sin(\mathbf{B}\cdot\mathbf{Q}/\phi_0), \tag{3.30}$$

where ϕ_0 is the (electromagnetic) flux quantum, $\mathbf{Q}$ is the (oriented, real space) area of the triad, and $\{\epsilon_j\}_{j=1}^3$ are the energies of the three single-particle eigenstates, which are invariant under reversal of the AB flux. The explicit expression for G can be found by substituting Eqs. (3.28a), (3.28b), (3.29a), and (3.29b) into Eqs. (3.18) and (3.3). (Note that in generic case G also depends on the populations of these states, which themselves may depend on particle-particle correlations.)

In Ref. 23, Holstein mainly addressed the issue of the Hall effect in hopping conductors in the presence of an ac electric field. Compared to the dc Hall effect, the ac problem is simplified because the principal contribution to the Hall conductance comes from those spatially isolated configurations of sites for which the population relaxation time $t_{\rm r}$ is on the order of the inverse frequency ω of the current (i.e., $\omega t_{\rm r}\sim 1$). In this ac case, there is no need to address the (highly nontrivial) issue of how these sources of the Hall effect (i.e., configurations of sites) are combined into a conducting network that is connected to the Hall contacts. For the dc Hall effect, on the other hand, this issue of the structure of the conducting network must be faced, and it becomes necessary to understand which triads are the most effective in contributing to the Hall effect, how to average over triads, and what quantity should be averaged. [If the quantity to be averaged should be the conductivity (resistivity) then one should first compute the local conductivities (resistivities) of triads and then obtain the macroscopic conductivities (resistivities) by averaging.] This issue of averaging over all triads and conducting network structure in disordered systems remains controversial.[75,76]

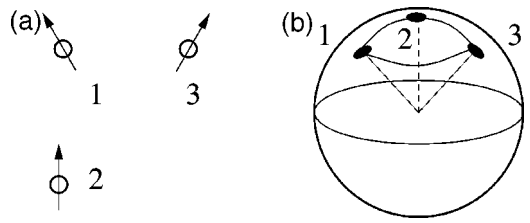

FIG. 14. (a) Triad of Mn ions having distinct core spin orientations. (b) Sphere of possible core spin orientations, showing the specific orientations of the spins for this triad. The orientations form the vertices of spherical triangle. The area of this triangle determines the quantal Pancharatnam phase.

However, in the present paper we are concerned not with the ordinary Hall effect in a system with localized carriers but the anomalous one. For the anomalous Hall effect, the Aharonov-Bohm phase does not play a fundamental role, a very weak magnetic field being applied solely for the purpose of inducing a macroscopic magnetization of a ferromagnetic medium. Rather, for the AHE in system comprising magnetically disordered core spins on Mn sites visited by hopping charge carriers, it is a certain type of *spin* quantal phase[47–49] that manifests itself. We now turn to the origin and meaning of this spin quantal phase.

E. The quantal Pancharatnam phase

To understand the nature of the spin quantal phases, let us begin by examining the single-particle quantum mechanics of a carrier hole added to a triad of Mn^{3+} ions. We regard the spin-3/2 core spins of the Mn ions as large enough to be treated classically, so that one can assign a definite direction to each of them. Thus, a generic configuration of core spins is characterized by the triad of unit vectors $\{\mathbf{n}_1,\mathbf{n}_2,\mathbf{n}_3\}$, respectively located at the triad of sites $\{\mathbf{R}_1,\mathbf{R}_2,\mathbf{R}_3\}$, as depicted in Fig. 14. Let us now consider the transfer of the hole carrier between ions. In the double exchange model, such transfer is described by the Hamiltonian

$$H_{\rm DE}=\sum_{\alpha,j}|\alpha,\phi_j\rangle\epsilon_j\langle\alpha,\phi_j|+\sum_{\substack{\alpha\\ j\neq k}}|\alpha,\phi_j\rangle V_{jk}\langle\alpha,\phi_k|$$
$$+J\sum_{\substack{\alpha,\beta\\ j}}|\alpha,\phi_j\rangle\mathbf{n}_j\cdot\boldsymbol{\sigma}_{\alpha,\beta}\langle\beta,\phi_j|, \tag{3.31}$$

where $\boldsymbol{\sigma}$ is the Pauli spin operator describing the spin of the hole carrier, J is the Hund Rules coupling energy which, for Mn^{3+} ions, is on the order of several eV, and is much larger than the orbital transfer integrals V_{jk}, and $|\alpha,\phi_j\rangle$ is the outer-shell atomic carrier state at site j, the index α labeling the spin-projection on to the z axis (i.e., $|\alpha\rangle|_{\alpha=\pm}$ are eigenstates of σ_z). In general, the Hamiltonian (3.31) results in spin polarization of electrons at arbitrary ratio of J and V_{jk}. However, two limiting cases are of interest. At $J\ll|V_{jk}|$, metallic ferromagnetism is usually treated perturbatively in terms of an electron gas in metals, resulting in the RKKY interaction. In this case charge carriers with any spin projection are taken into account. The opposite case $J\gg|V_{jk}|$ is a

purely double-exchange model. This is the case that is relevant to manganites. By Hund's rules (appropriate for $J \gg |V_{jk}|$), there is, at each site, effectively a single quantum state available to the hole. This state $|\mathbf{n}_j, \phi_j\rangle$ is the one in which the carrier spin projection opposes the core spin direction. The orbital $|\phi_j\rangle$ that characterizes this state is *one* of the orbitals of an isolated Mn ion, centered on the site *j*; we choose to omit the remaining orbitals so as to simplify the discussion. As for the other spin state (as well as any other orbitals), we regard them as being inaccessible on energetic grounds. Postponing until later any effects of spin-orbit interactions, we assume that the transfer of carriers [being, as it is, affected by either the ''kinetic energy,'' by the second term in Eq. (3.31), or by the electron-phonon interaction] has no effect on the spin of the carriers. The hopping amplitudes between ionic states are thus given by $\langle \mathbf{n}_k, \phi_k | T | \mathbf{n}_j, \phi_j \rangle$, where T corresponds either to the transfer operator V of Eq. (3.7) or to the electron phonon interaction $H_{\text{el-ph}}$. These hopping amplitudes depend explicitly on the relative orientation of the core spins, $\mathbf{n}_k$ and $\mathbf{n}_j$. In particular, by projecting the Hamiltonian (3.31) on to the physically relevant low-energy subspace spanned by the states $|\mathbf{n}_j, \phi_j\rangle$, we arrive at the the double-exchange Hamiltonian projected on to the low-energy subspace, H'_{DE}, which takes the form

$$H'_{\text{DE}} = \sum |\mathbf{n}_j, \phi_j\rangle (\epsilon_j - J) \langle \mathbf{n}_j, \phi_j| + \sum_{j \neq k} |\mathbf{n}_j, \phi_j\rangle V^{\text{eff}}_{jk} \langle \mathbf{n}_k, \phi_k|, \tag{3.32a}$$

$$\begin{aligned} V^{\text{ef}}_{jk} &\equiv \langle \mathbf{n}_j, \phi_j | H_{\text{DE}} | \mathbf{n}_k, \phi_k \rangle \\ &= V_{jk} \left(\cos\frac{\theta_j}{2} \cos\frac{\theta_k}{2} + e^{i\gamma_{kj}} \sin\frac{\theta_j}{2} \sin\frac{\theta_k}{2} \right), \end{aligned} \tag{3.32b}$$

where V^{ef}_{jk} are the effective transfer amplitudes, $\gamma_{kj} \equiv \gamma_k - \gamma_j$ and, respectively, θ_j and θ_k are the azimuthal angles and γ_j and γ_k are the polar angles of the semiclassical spin directions $\mathbf{n}_j$ and $\mathbf{n}_k$. Provided we choose, e.g., $\mathbf{n}_j \| \mathbf{e}_z$ and $\mathbf{n}_k \| \mathbf{e}_x$ (where $\{\mathbf{e}_x, \mathbf{e}_y, \mathbf{e}_z\}$ are the Cartesian basis vectors) this effective transfer amplitude reduces to the Anderson-Hasegawa form

$$V^{\text{AH}}_{jk} = V_{jk} \cos\theta/2, \tag{3.33}$$

where θ is the angle between $\mathbf{n}_j$ and $\mathbf{n}_k$. However, and this is central to our discussion, the effective transfer amplitude is, in general, a complex quantity characterized by its amplitude and phase. From Eqs. (3.32b) and (3.33), it is indeed apparent that if core spins are co-aligned, the effective hopping amplitude is maximal, while if the core spins on two ions are opposite, hopping between such ions does not occur.

We now follow the line of argument applied in Sec. III D 3, and construct the exact eigenstates of Hamiltonian (3.32a), via Eq. (3.13) modified to account for spin. Hence, we can build matrix elements of the electron-phonon interaction between exact localized states, taking into account the effect of the core spin orientations $\{\mathbf{n}_j\}$. We now note that this expansion for the state gives rise, in the hopping probability $|U_{ji}|^2$ (and hence in the hopping rate W_{ji}), to terms containing products of matrix elements such as transfer integrals V^{eff}_{kj} and electron-phonon interactions U_{kj}. Amongst these terms are ones containing matrix elements associated with paths around closed loops and incorporating the effects of interference between distinct carrier paths. The simplest example involves the product $V^{\text{eff}}_{ij} V^{\text{eff}}_{kj} V^{\text{eff}}_{ji}$, associated with the path $i \to j \to k \to i$.

In the presence of the constraints set by the core spin orientations, the transfer of carriers discussed in the previous paragraph is subject to a striking quantal effect. To see this, consider the products of matrix elements $V^{\text{eff}}_{ik} V^{\text{eff}}_{kj} V^{\text{eff}}_{ji}$. Explicitly, such products have the form

$$\begin{aligned} V^{\text{eff}}_{ik} V^{\text{eff}}_{kj} V^{\text{eff}}_{ji} &= \langle \mathbf{n}_i, \phi_i | H_{\text{DE}} | \mathbf{n}_k, \phi_k \rangle \langle \mathbf{n}_k, \phi_k | H_{\text{DE}} | \mathbf{n}_j, \phi_j \rangle \\ &\quad \times \langle \mathbf{n}_j, \phi_j | H_{\text{DE}} | \mathbf{n}_i, \phi_i \rangle \\ &= \langle \mathbf{n}_i | \otimes \langle \phi_i | H'_{\text{DE}} | \phi_k \rangle \otimes | \mathbf{n}_k \rangle \\ &\quad \times \langle \mathbf{n}_k | \otimes \langle \phi_k | H'_{\text{DE}} | \phi_j \rangle \otimes | \mathbf{n}_j \rangle \langle \mathbf{n}_j | \\ &\quad \otimes \langle \phi_j | H'_{\text{DE}} | \phi_i \rangle \otimes | \mathbf{n}_i \rangle \\ &\propto \langle \mathbf{n}_i | \mathbf{n}_k \rangle \langle \mathbf{n}_k | \mathbf{n}_j \rangle \langle \mathbf{n}_j | \mathbf{n}_i \rangle = \text{Tr}\, P_k P_j P_i, \end{aligned} \tag{3.34}$$

where the operators $P_j \equiv (1 + \boldsymbol{\sigma} \cdot \mathbf{n}_j)/2$ are projectors (in spin space) on to the spin states aligned with the local core spin orientations $\mathbf{n}_j$. From this last expression, in terms of projectors, it is straightforward to establish that

$$\text{Tr}\, P_k P_j P_i = (1 + \mathbf{n}_1 \cdot \mathbf{n}_2 + \mathbf{n}_2 \cdot \mathbf{n}_3 + \mathbf{n}_3 \cdot \mathbf{n}_1) + i[\mathbf{n}_1 \cdot (\mathbf{n}_2 \times \mathbf{n}_3)]. \tag{3.35}$$

Hence, we arrive at the quantal phase Ω, the phase of the complex quantity $\text{Tr}\, P_k P_j P_i$, which is given by

$$\frac{\Omega}{2} = \tan^{-1} \frac{\mathbf{n}_1 \cdot (\mathbf{n}_2 \times \mathbf{n}_3)}{1 + \mathbf{n}_1 \cdot \mathbf{n}_2 + \mathbf{n}_2 \cdot \mathbf{n}_3 + \mathbf{n}_3 \cdot \mathbf{n}_1}. \tag{3.36}$$

In the context of the physical quantity from which the computation of the quantal phase Ω emerged, viz., the perturbative evaluation of the hopping rate W_{kj}, Eq. (3.18), this phase modulates the interference between hopping processes that progress from one site *j* to another site *k*, either directly or indirectly, via a third site.

Formula Eq. (3.36) indicates that the phase Ω has a geometric interpretation as the (oriented) solid angle of the geodesic triangle having vertices at $\{\mathbf{n}_i, \mathbf{n}_j, \mathbf{n}_k\}$ on the unit sphere. It is the quantal analog of the classical optical phase discovered in the context of polarized light by Pancharatnam.[25,26] In that setting, what Pancharatnam showed is that a under a sequence of changes of the polarization state of light that return the light to its original polarization state there arises a phase shift (i.e., a phase anholonomy) determined by the geometry of the sequence of changes. If the sequence of polarization states is represented by a sequence of points on the Poincaré sphere (a certain parametrization of light polarizations) then Ω is given by the area of the geodesic polygon on this sphere the vertices of which are correspond to these polarization states.

In the double-exchange electronic analog of Pancharatnam's phase, the transporting of an outer-shell carrier to an

ion with a differently oriented core spin via a spin-independent process is characterized by a matrix element that can be interpreted as a *connection*. For processes visiting a closed sequence of sites, this connection yields a quantal phase Ω, viz., the phase shift of the returning spin state in terms of the sequence of sites visited. This quantal version of Pancharatnam's phase is given by *half* the area of the geodesic polygon (on the unit sphere of core spin orientations) the vertices of which are the core spin orientations of the sites visited. Although the phase Ω emerged from considerations of interference between processes involving a *triad* of sites, such phases are more general and would, in fact, emerge for arbitrary processes. We remark that, in contrast to Berry's adiabatic phase,[51] the phenomenon described here is associated with *sudden* changes in the carrier-spin state, and need not be slow.

F. The anomalous Hall effect in hopping regime

We now turn from the OHE in a spinless triad to the AHE in a triad of magnetic sites. Like the OHE given by Eq. (3.30), this AHE results from two-phonon processes, but is due to the Pancharatnam phase instead of the AB phase. (At this stage, we have not yet included the effects of the spin-orbit interaction.) *Mutatis mutandis*, we arrive at the AH conductivity $\sigma_{\rm AH}$, given by

$$\sigma_{\rm AH} = G\{\varepsilon_j\} \cos\frac{\theta_{13}}{2} \cos\frac{\theta_{32}}{2} \cos\frac{\theta_{21}}{2} \sin\frac{\Omega}{2}, \qquad (3.37)$$

where $\cos\theta_{jk} \equiv \mathbf{n}_j \cdot \mathbf{n}_k$, the factors $\cos(\theta_{jk}/2)$ are Anderson-Hasegawa factors, and $\{\varepsilon_j\}$ are the energies of the three on-site single-particle eigenstates that are consistent with Hund's rules, these energies depending on $\{\mathbf{n}_j \cdot \mathbf{n}_k\}_{1 \leqslant j < k \leqslant 3}$ and $\cos(\Omega/2)$. Note that G is even under the reversal of the Pancharatnam flux $\Omega \to -\Omega$, and $\sigma_{\rm AH}$ is odd under it.

We have shown that, for a triad with given set of core-spin orientations, an AHE arises from the quantal Pancharatnam flux. However, there is a significant difference between this AHE and the OHE. In the former (nonmagnetic) case, a uniform applied magnetic field leads to a net macroscopic OHE, even though contributions of triads may cancel one another.[75] In the latter case (with its magnetic sites, Pancharatnam flux, but spin-orbit interactions not yet included), even the presence of a macroscopic magnetization of the core spins is insufficient to cause a *macroscopic* Hall current. The reason for this is that in obtaining the macroscopic AH current from Eq. (3.37) we must average over the configurations of the core spins. In the absence of spin-orbit interactions, the distribution of these configurations, although favoring a preferred *direction* (i.e., the magnetization direction $\mathbf{m} \equiv \mathbf{M}/M$), is invariant under a reflection of all core-spin vectors in any plane containing the magnetization, and, therefore, there is no preferred Pancharatnam flux. For example, two spin configurations shown in Fig. 15 have the same magnetization but opposite signs of the Pancharatnam flux. This fact, coupled with the fact that $\{\varepsilon_j\}$ are also invariant under such reflections, guarantees that the macroscopic AH current will average to zero. [We do, however, expect significant AH current *noise* in the ferromagnet-paramagnet transition regime, owing to the fluctuations of the Pontryagin charge[77] of the triads of core spins (which we shall define shortly) and, hence, elementary Pancharatnam fluxes.]

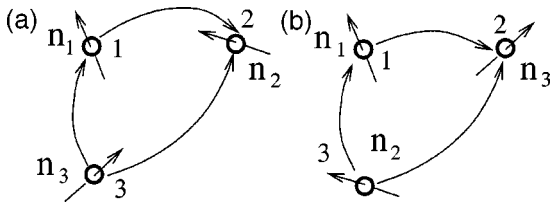

FIG. 15. Two configurations [(a) and (b)] of core spins on a triad of Mn ions, differing by the interchange of the spins on sites 2 and 3. These distinct spin configurations give rise to opposite Pancharatnam phases.

In order to capture the AHE in double-exchange materials such as manganites, we must consider not only the Pancharatnam phase but also some agent capable of lifting the reflection invariance of the energies $\{\varepsilon_j\}$ and the distribution of core-spin configurations and, hence, capable of inducing sensitivity to the sign of the Pancharatnam flux. Such an agent is provided by spin-orbit interactions. We now discuss the effect of these interactions on the motion of charge carrier in a triad.

G. Spin-orbit interactions in a triad

The most general form of spin-orbit interaction is given by the spin-orbit Hamiltonian

$$H_{\rm so} = \alpha \mathbf{p} \cdot (\boldsymbol{\sigma} \times \boldsymbol{\nabla} U), \qquad (3.38)$$

where the potential U includes ionic and impurity potentials, α is the spin-orbit interaction constant, $\mathbf{p}$ is the electron momentum, and $\boldsymbol{\sigma}$ are the Pauli operators. This spin-orbit interaction results in an effective SU(2) gauge potential $\mathbf{A}_{\rm so} = \alpha m(\boldsymbol{\sigma} \times \boldsymbol{\nabla} U)$,[78] where m is the relevant mass of the carrier. This gauge potential provides an additional source of quantal phase. For a given core-spin configuration, the spin-orbit interaction favors one sense of carrier-circulation around the triad over the other, and thus favors one sign of Pancharatnam phase over the other.

Let us consider the consequences for the energy spectrum of the triad $\{\varepsilon_j\}$ that arise due to spin-orbit interactions. This interaction generates a dependence of $\{\varepsilon_j\}$ on the three vector products $\mathbf{N}_{jk} \equiv \mathbf{n}_j \times \mathbf{n}_k$ which, together with the magnetization direction $\mathbf{m}$, yield a preferred value for the triad Pontryagin charge $q_{\rm P}$ $[\equiv \mathbf{n}_1 \cdot (\mathbf{n}_2 \times \mathbf{n}_3)]$ and, hence, a preferred Pancharatnam flux.

It is straightforward to find corrections, due to the SOI, of hole eigenenergies if the on-site energies of the holes are nondegenerate. Then the sensitivity of $\{\varepsilon_j\}$ to vector products $\mathbf{N}_{jk} \equiv \mathbf{n}_j \times \mathbf{n}_k$ first enters at third order (in the transfer matrix elements),

$$\delta\varepsilon_j = \sum_{h,k(\neq j)} {\rm Tr}\, T_{jh} T_{hk} T_{kj} / (\varepsilon_j - \varepsilon_h)(\varepsilon_j - \varepsilon_k), \qquad (3.39)$$

where $T_{jk} \equiv P_j V_{jk} P_k$ are the transfer amplitudes, V_{jk} are the hopping matrix elements, and Tr denotes a trace in spin

space. (For degenerate on-site hole energies one should obtain the splitting of these energies due to transfer in the absence of SOI, and then include SOI at the final step, arriving at the result to be given below.) The hopping matrix elements are sensitive to the SOI quantal phase, and can be written in the form $V_{jk}=V_{jk}^{\rm orb}L_{jk}$, where $L_{jk}\equiv(1+i\boldsymbol{\sigma}\cdot\mathbf{g}_{jk})$, $V_{jk}^{\rm orb}$ is an orbital factor, and $\mathbf{g}_{jk}$ ($\propto\alpha_{\rm so}$) is an appropriate vector that describes the average SOI for the transition $j\rightarrow k$ in a triad of sites i, j, and k. Then, e.g., the first-order (in α) shifts in the ε's are given by

$$\begin{aligned}\delta\varepsilon_j &\propto \mathrm{Tr}\, T_{13}T_{32}T_{21}\\ &= 4\ \mathrm{Re}\,\mathrm{Tr}\, P_1L_{13}P_3L_{32}P_2L_{21}\\ &= 2(\mathbf{N}_{13}\cdot\mathbf{g}_{13}+\mathbf{N}_{32}\cdot\mathbf{g}_{32}+\mathbf{N}_{21}\cdot\mathbf{g}_{21})-\mathbf{N}\cdot\mathbf{g},\end{aligned} \tag{3.40}$$

where $\mathbf{N}\equiv\mathbf{N}_{13}+\mathbf{N}_{32}+\mathbf{N}_{21}$, and $\mathbf{g}\equiv\mathbf{g}_{13}+\mathbf{g}_{32}+\mathbf{g}_{21}$. If the potential U in the SOI is a superposition of spherically-symmetric ionic potentials in a the triad of sites then the vectors $\mathbf{g}_{jk}$ have a transparent geometrical meaning:

$$\mathbf{g}_{jk}=a_{jk}\mathbf{Q}, \tag{3.41}$$

$$\mathbf{Q}=\frac{1}{2}(\mathbf{R}_j-\mathbf{R}_h)\times(\mathbf{R}_k-\mathbf{R}_h), \tag{3.42}$$

i.e., they are proportional to the area $|\mathbf{Q}|$ of the triangle whose vertices are the sites $\mathbf{R}_j$, $\mathbf{R}_k$ and $\mathbf{R}_h$. Then the SOI-generated shift in the carrier eigenenergies has the Dzyaloshinski-Moriya form.[27]

H. Elementary Hall conductivity in a triad

There are two contributions to the AHE which result from the SOI-generated shift in the carrier eigenenergies. The first contribution is due to the dependence of the probability of hopping around the triad on $\{\varepsilon_j\}$ for a given spin configuration. By incorporating the shifts (3.40), together with the Pancharatnam phase, we arrive at the elementary AH conductivity

$$\sigma_{\rm AH}^{(1)}=\mathbf{n}_1\cdot(\mathbf{n}_2\times\mathbf{n}_3)\sum_j\ \delta\varepsilon_j\partial G/\partial\varepsilon_j\,. \tag{3.43}$$

As discussed above, Eq. (3.43) has a nonzero macroscopic average, owing to the presence of a characteristic Pontryagin charge constructible from the $\mathbf{N}_{jk}$, that feature in the energy shifts, and the magnetization direction. A second consequence of the SOI-generated carrier-energy shift (3.40) leads to the second contribution, $\sigma_{\rm AH}^{(2)}$. Due to the feedback of the (fast) carrier freedoms, which provide an effective potential for the (slow) spin system, determined by Eq. (3.40), the equilibrium probabilities of spin configurations having opposing Pancharatnam fluxes will no longer be equal. (For this contribution, which is related not to $\partial G/\partial\varepsilon_j$ but to G itself, there is no need to account for SOI-induced carrier-energy shifts in the current now being averaged over a non-symmetric spin-configuration distribution.) A contribution with this origin has also been considered in Ref. 29. $\sigma_{\rm AH}^{(1)}$ and $\sigma_{\rm AH}^{(2)}$ are of the same order of magnitude.

I. Structure of the conducting network and the AHE resistivity

We now consider the question of how the physics of elementary triads of Mn ions relates to the macroscopic properties of manganites. For hopping conductivity, the pathways taken by the current depends sensitively on the details of the configuration of the core spins, owing to the sensitivity of the hopping amplitudes to the core-spin alignments. In particular, regions having local spin configurations that are aligned roughly opposite to the macroscopic magnetization of the sample tend to be avoided by the current. This fact renders rather subtle the procedure for averaging over equilibrium spin configurations, which must account for effects such as local spin correlations and excitations of various types (i.e. spin wave and topological excitations).

En route to computing the AH resistivity, let us try to identify through which triads the AH current tends to flow. Carriers tend to pass through regions of lower resistance. However, currents through regions with aligned spins do not lead to an AHE because the relevant Pancharatnam flux through such regions is small. Furthermore, in the ferromagnet-to-paramagnet transition region, where the magnetization is only a small fraction of its saturation value, even those spins within the network responsible for longitudinal conductivity have orientations that are typically splayed, relative to one another. Nevertheless, if one were to consider only the spins in this network, their average magnetization would be larger than that of the entire sample, and the typical solid angles formed by triads of such spins would be rather small. Thus, any AHE originating in such triads would be not the dominant contribution. Moreover, close to the metal-insulator transition, hopping paths through the sample that encounter spins having rather common orientations do not exist.

In fact, there is experimental evidence for the existence of moderately sized clusters of aligned spins coming from neutron scattering data[61,79] at temperatures near the ferromagnet-to-paramagnet transition. These data indicates that clusters of spins do indeed exist in which spins are aligned over a length scale of roughly 10 Å. Thus, it is reasonable to envision the magnetic configurations as comprising rather well oriented clusters of, say, twenty to thirty spins, with adjacent clusters having rather different spin orientations. Furthermore, theoretical estimates of the scale of magnetic fields relevant for colossal magnetoresistance are consistent with the existence of such clusters. (Such clusters can be regarded as being large magnetic polarons.[80]) As the characteristic Zeeman temperature associated with a *single* spin-3/2 in a magnetic field of 7 T is 20 K, whereas the characteristic temperature associated with colossal magnetoresistance is roughly 200 K, one is lead to the view that clusters of correlated spins involve on the order of ten spins.

Now consider two adjacent clusters of roughly aligned spins [e.g., clusters L and R in Fig. 16(a)]. Even the conducting paths connecting these clusters contain bonds between

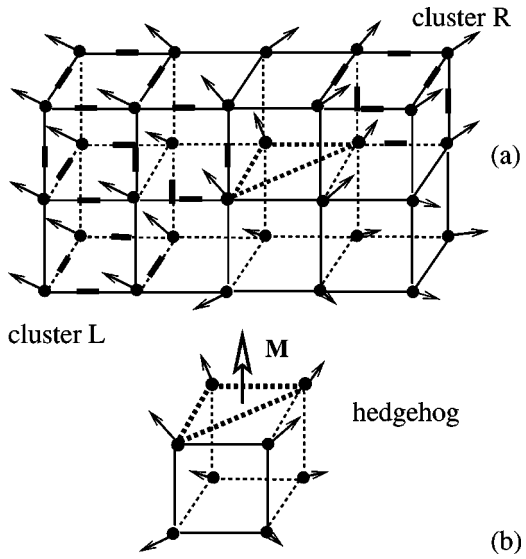

FIG. 16. (a) Two clusters of sites, denoted *L* and *R*, in a fragment of the sublattice of Mn sites. Within a cluster the core spin orientations are roughly the same; but spins in distinct clusters have significantly different orientations. Note that the boundary between such clusters is liable to contain spin configurations that resemble the single hedgehog configuration shown in (b). The heavy dotted lines in (a) indicate a triad of spins that contribute to a hedgehog configuration. Sites in the upper part of the cell shown in (b) contribute to the conducting network and, correspondingly, the magnetization (per site) in this upper part of the cell (shown as an open-headed arrow) is roughly that of the sample (see the discussion in Sec. III I).

ions having significantly misaligned spins. These spins belong to regions of magnetic inhomogeneity, e.g., inhabited by hedgehog excitations [an example of ''lattice hedgehog'' is shown in Fig. 16(b)] which defines the border of aligned clusters as shown in Fig. 16(a). As mentioned in the Introduction, hedgehog excitations are long-lived topological spin excitations, the existence of which is known to be important for ferromagnet-to-paramagnet transition,[53,57] even in the three dimensional case.

Within these regions of magnetic inhomogeneity there are triads of splayed spins. Let us now address the question: What is the characteristic splay? To answer this question, imagine dividing up the spins into those within clusters and those within the border regions. Even though the magnetization per spin in a typical cluster is greater than the sample-average magnetization per spin, the clusters are misoriented relative to one another. Thus the contribution to the magnetization per spin of the sample coming from the spins in clusters is not guaranteed to exceed the sample average and, indeed, it seems reasonable to assume that it is, in fact, not so different from the sample average. If so, then the magnetization per spin of the spins in the border region would also be roughly the sample average. We shall make the hypothesis that this is indeed the case. Then the magnetization of typical triads of ions in the border region can also roughly be taken to be the average sample magnetization. We shall denote by β the characteristic angle that spins in a triad form with the direction of the overall magnetization of the sample **M**: $\cos\beta \sim |\mathbf{M}|/M_s$, where M_s is the saturation magnetization of the sample.

Let us now imagine how charge carriers move between clusters having quite different ion spin orientations. Such motion is necessary for the existence charge-carrier propagation between electrical contacts. We have sketched a typical instantaneous configuration of the spins in Fig. 16. As one can see, the ''upper'' part of a inhomogeneous region formed on a cubic lattice of sites can serve as a path for hopping between clusters. For reasons that we will now give, triads of sites within this (and similar) regions are effective contributors to the AHE.

(i) The three spins in the triad have positive components along the direction of magnetization. (Recall that clusters with magnetization pointing against the majority tend to be avoided by the current.) This allows participation by these triad sites in the conducting network. If all three sites participate in the conducting network, the triad can be an effective source of an electromagnetic force that leads to a Hall effect. As we have discussed, the net magnetization of the triad is roughly that of the bulk, which makes it magnetically compatible with its neighbors.

(ii) Typical triads of spins, being located as they are between several misoriented clusters are significantly splayed. Therefore, the solid angle formed by their spins (i.e., the area of the geodesic triangle formed by their orientations on the unit sphere, also known as the Pontryagin charge of the spin configuration) is substantial and, in fact, close to the maximum possible value given the constraint that the triad magnetization (per spin) be comparable to the sample magnetization (per spin). Thus, we adopt as a caricature of the spin configuration in regions contributing to the Hall effect a picture of splayed triads of spins of known magnetization density, residing within tetrads of spins on a lattice plaquette, such as those depicted by the lattice hedgehog configuration shown in Fig. 16. This scheme, in which we consider tetrads of a given magnetization and then select triads of sites in a tetrad, seems to us appropriate, given the cubic structure of the sublattice of Mn spins. However, alternative schemes (e.g., in which one considers triads themselves or other assemblies of splayed spins of a given magnetization rather than tetrads, and chooses triads out of these assemblies) lead to almost identical results (e.g., for the scaling of the Hall resistivity, which we discuss in the present and following sections). This insensitivity to details is all the more natural, given that we are dealing with an atomically disordered system. We note that, because hedgehogs are topologically stable, they provide a mechanism by which the spin configuration can sustain strongly splayed regions that persist for durations much longer than the characteristic time for charge motion. Hence, in their presence, on can accurately treat the charge motion as taking place with a background of inhomogeneous but essentially static spins, which renders consistent the adiabatic treatment of the dynamics of the spins.

Thus, we arrive at the notion of an *optimal triad.* An optimal triad is a triad of spins residing in a tetrad of four spins around a plaquette of the cubic sublattice of Mn ions and having the following properties: (i) The tetrad has the

magnetization density of the bulk; and (ii) subject to this constraint, the spins of the tetrad are maximally splayed (i.e., subtend the maximal solid angle and, in fact, are configured symmetrically around a cone). Note that if the lattice were triangular then we would simply have adopted a definition of optimality in terms of maximally splayed triads (rather than tetrads) of spins. As mentioned above, in disordered systems (such as manganites), the distinctions engendered by such options are unlikely to have a strong impact on the physical consequences of the picture.

The motion of charge carriers through optimal triads gives rise to the AHE. We note that these optimal triads have properties quite different from those of optimal triads contributing to the OHE in doped, nonmagnetic semiconductors:[75] in the OHE setting, only two sites in an optimal OHE triad are connected to the conducting network, whereas in the optimal AHE triads all three triad sites participate in the network. (Indeed, if alternatively, one of the sites is *not* a part of the conducting network, its spin must be roughly opposite that of the spins on the other two sites; such a configuration would yield only a small Pancharatnam phase.)

The question may arise why triads within tetrads (and not, for instance, tetrads themselves) are considered to be the dominant source of the AHE. By a contribution from a tetrad we mean one involving four overlap integrals. As these overlap integrals are small, owing to the localized character of the carrier wavefunctions and, thus, the contribution from tetrads is suppressed, relative to that from triads. We note that distortions due to doping, particularly deviations of Mn-O-Mn bond angles from 180°, facilitates tunneling between Mn ions via plaquette diagonals (see Fig. 16). As was estimated in Ref. 4, the amplitude of transfer along diagonals is 0.5 of that between nearest neighbor Mn ions. Recent tight binding model parametrization of local density approximation (LDA) studies[81] show that hopping via diagonals is even more important, and its amplitude is 0.82 of transfer amplitude between nearest neighbor Mn ions.

Having discussed the structure of resistive network, let us now calculate the longitudinal and Hall resistivities of manganites in the regime in which conductivity proceeds by hopping (i.e., at temperatures above, as well as somewhat below, the ferromagnet-to-paramagnet transition). The longitudinal hopping conductivity arising from phonon-assisted hops between sites i and j is given by

$$\sigma_{xx}=(ne^2d^2/k_BT)W_0^{ij}\cos^2(\theta/2), \tag{3.44}$$

[cf. Eqs. (3.1) and (3.2b)], where d is the distance between sites. Here, W_0^{ij} is the rate of phonon-assisted direct hops, and we have explicitly separated out the Anderson-Hasegawa factor $\cos^2(\theta/2)$. Correspondingly, the (anomalous) Hall conductivity is given by [cf. Eq. (3.3)]

$$\sigma_{xy}=(ne^2d^2/k_BT)W_1^{ij}, \tag{3.45}$$

where W_1^{ij} is the rate of hopping between the two sites, and accounts for interference associated with both direct hopping and hopping via an intermediate state on a third site. Note that the quantity W_1 includes three Anderson-Hasegawa factors [and so does the Hall conductivity given by Eq. (3.37)]. The task of computing the Hall resistivity ρ_{xy}, which in the limit of $\sigma_{xx}\gg\sigma_{xy}$ under consideration has the form

$$\rho_{xy}\approx-\frac{\sigma_{xy}}{\sigma_{xx}^2}, \tag{3.46}$$

then reduces to a determination of a ratio involving the direct and indirect hopping rates W_0^{ij} and W_1^{ij} (as a function of the magnetization texture). As discussed in Secs. III D and III F, W_1^{ij} involves two-phonon processes, whereas W_0^{ij} involves only single-phonon processes. Because of this, dependence on electron-phonon coupling constant, phonon occupation numbers, and charge carrier occupation numbers, cancels from the relevant ratio, $W_1^{ij}/(W_0^{ij})^2$, so that this ratio can be written as

$$W_1/W_0^2=\alpha\hbar\zeta/k_BT, \tag{3.47}$$

where α is a numerical factor describing the multiplicity of the various carrier-phonon interference processes (see Ref. 23 and Sec. III D), the number of intermediate sites, and the difference between nearest- and next-nearest-neighbor hopping amplitudes. We shall refer to the parameter ζ, which characterizes the difference between the forward W_1^{ij} (backward W_1^{ji}) transition rates, as an asymmetry parameter. For the OHE, this asymmetry parameter is given by

$$\zeta\propto\sin(\mathbf{B}\cdot\mathbf{Q}/\phi_0), \tag{3.48}$$

where $\mathbf{Q}$ is the vector area defined in Eq. (3.42), as follows from Eq. (3.3).

For the AHE, it follows from Eqs.(3.40) and (3.43) that the asymmetry parameter is given by

$$\zeta\simeq 3[\mathbf{g}_{jk}\cdot(\mathbf{n}_j\times\mathbf{n}_k)][\mathbf{n}_1\cdot(\mathbf{n}_2\times\mathbf{n}_3)]/4, \tag{3.49}$$

where $\mathbf{g}_{jk}$ are characteristic vectors arising in the hopping amplitude owing to the spin-orbit quantal phase; $\mathbf{n}_j$ are unit vectors of the core spins in the triad, and $\mathbf{n}_1\cdot(\mathbf{n}_2\times\mathbf{n}_3)$ is the volume of a parallelepiped defined by core-spin vectors, i.e., the Pontryagin charge q_P. The anomalous Hall resistivity can be written in the simple form

$$\rho_{xy}\simeq-\sigma_{xy}/\sigma_{xx}^2=-\frac{1}{ne}\left(\frac{\alpha\hbar\zeta}{ed^2}\frac{1}{\cos^4(\theta/2)}\right). \tag{3.50}$$

The evaluation of Eq. (3.50) reduces to a determination of θ, along with the products $(\mathbf{n}_j\times\mathbf{n}_k)$ and $\mathbf{n}_1\cdot(\mathbf{n}_2\times\mathbf{n}_3)$, which survive averaging over all possible triads. The dominant contribution to the average of these products arises from optimal spin configurations (see Fig. 17).

Therefore, in line with properties (i) and (ii) of these configurations, consider a square lattice formed by the Mn ions in a plane perpendicular to $\mathbf{m}$ [as in, e.g., the top surface of the cube in Fig. 16(b)]. To ascertain the geometry of optimal triads, consider the spins at four sites of a plaquette belonging to the conducting network. Being optimally configured, these spins lie at equal separations around a cone whose vertical angle 2β is given by $2\cos^{-1}[M(H,T)/M_{sat}]$. (The angle between the altitude of the cone and any generator in

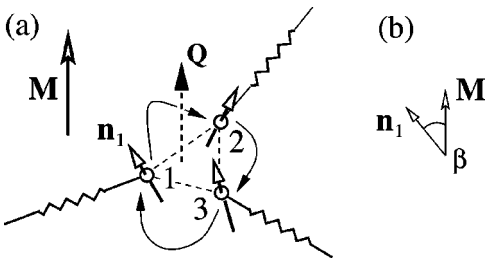

FIG. 17. (a) Triad of Mn sites (1, 2 and 3) in the conducting network. Charge-carrier motion around triads such as this lead to the AHE. We compute the longitudinal and AH conductivities by relating them to the configuration of the spins (which we suppose to be optimal) and, hence, to the magnetization.

the conical surface is β.) Let us now use this information to fix the various geometrical quantities that determine the longitudinal and Hall conductivities, the former being associated with pairs of sites and the latter with triads. We assert that to compute the contributions to these conductivities we may consider sites in an optimal configuration, as these are characteristic of that regions of the sample that dominantly contribute. For the Hall conductivity, the reasons for accepting this assertion were discussed in the present subsection. As for the longitudinal resistivity, the assertion is valid because this quantity is dominated by the most resistive regions of the conducting network, and these are expected to arise at the interface between clusters of aligned spins, i.e., in regions that are hedgehog-like.

With this picture in mind, we now compute characteristic values for the geometrical quantities that feature in the longitudinal and Hall conductivities. Thus, we need the angle θ between adjacent spins, the Pontryagin charge q_{P}, and the products $(\mathbf{n}_j \times \mathbf{n}_k)$, each of which is related to the vertical angle 2β by elementary geometry:

$$2\cos^2(\theta/2) = 1 + \cos^2\beta, \tag{3.51a}$$

$$q_P = 2\cos\beta\sin^2\beta, \tag{3.51b}$$

$$\mathbf{m}\cdot(\mathbf{n}_j \times \mathbf{n}_k) = \sin^2\beta. \tag{3.51c}$$

We now have to account for the fact that, in the hopping regime, the magnitude of the longitudinal (and anomalous Hall) resistivities depend on the probability that pairs and triads of ions are connected to the conducting network. We introduce a percolation factor P describing the connectivity of the pair to the conducting network; for the AH conductivity the corresponding factor would be P^2 because both pairs of ions in a triad must, as discussed above, belong to the conducting network. It is remarkable that, throughout the localization regime, ρ_{xy} is nevertheless determined by currents formed in individual pairs and triads, because the factors of P cancel in the expression for ρ_{xy} given by Eqs. (3.46) and (3.50). Therefore, in so far as q_{P} and the angles between neighboring spins can be directly related to $m \equiv M/M_{\mathrm{sat}} = \cos\beta$, the Hall resistivity ρ_{xy} depends on H and T only through $m(H,T)$, and is given by

$$\rho_{xy} = \rho_{xy}^0 \frac{m(1-m^2)^2}{(1+m^2)^2}. \tag{3.52}$$

To determine the magnitude of the AHE, we first need to estimate the characteristic values of $|\mathbf{g}_{jk}| \sim g$ arising from the spin-orbit interaction (SOI). As discussed in Sec. III G, the SOI term leads to a Dzyaloshinski-Moriya contribution to the eigenenergy of the carriers. A standard estimate[82] gives the characteristic values of $|\mathbf{g}| \sim g \sim Ze^2/4m_e c^2 d_0$, where d_0 is the radius of an Mn core d state. While renormalization of carrier parameters in crystals may tend to increase $|\mathbf{g}_{jk}|$, crystalline symmetry requires admixtures of core orbitals, which, in turn, are mixed with oxygen p orbitals, with outer-shell wavefunctions in order to have $|\mathbf{g}_{jk}| \neq 0$. Such admixture is effectively generated by the non-collinearity of the Mn-O-Mn bonds that allows carrier hopping around triads (including jumps along plaquette diagonals). An estimate based on free electron parameters gives $g \sim 5 \times 10^{-4}$. (We note that band-structure calculation of the spin-orbit coupling constants is outside the scope of this paper.) The characteristic strength of the Dzyaloshinski-Moriya terms is $\sim g t_0 \sim 0.02$ meV, and the characteristic strength of the spin-orbit interaction is $\sim \epsilon t_0 \sim 0.1$ meV, where ϵ is the characteristic carrier energy. Not only these strengths are much smaller than the characteristic double exchange energy, but they are even smaller than the magnitude of the direct antiferromagnetic Heisenberg exchange term. However, for the anomalous Hall effect in the localized regime, the Dzyaloshinski-Moriya terms are crucial, as we discussed in Sec. III F.

We now estimate the macroscopic longitudinal and Hall resistivities in the regime in which the conducting network is fully connected, i.e., in the regime IV of Fig. 10. By taking $n = 5.6 \times 10^{21}$ cm^{-3}, $W_0 \sim 2.5 \times 10^{13}$ s^{-1}, and, from the magnetization data at $T = 275$ K (Fig. 1), $\cos\beta = 0.6$, we obtain $\rho_{xx} \simeq 1$ mΩ cm which coincides with the value of the experimentally observed resistivity for LPMO (see Fig. 3). The AHE contribution to the Hall resistivity, assuming a numerical factor α of 2.5, is then $\rho_{xy} \approx -0.5$ $\mu\Omega$ cm, in agreement with the experimentally observed LPMO Hall resistivity at the same T (Fig. 5). The equivalent expression for the hopping Hall resistance in the Holstein mechanism is defined by the asymmetry parameter $\zeta \simeq \cos^2(\theta/2)\cos\beta\sin(\mathbf{B}\cdot\mathbf{Q}/\phi_0)$ and, at $B = 1$ T, is an order of magnitude smaller than the AHE. We expect the macroscopic hopping AH and OH effects to have the same sign, opposite to that of the OHE in the metallic regime.

In the next section, Sec. IV, we shall compare the results for the Hall resistivity with the experimental data. As we shall see, the picture for the core spin configurations developed above, which include clusters of oriented spins and hedgehog-configured spins, allows us to explain not only the AHE, but ferromagnet-to-paramagnet and metal-insulator transitions in manganites, and provide a quantitative explanation of the magnitude of characteristic magnetic field that result in colossal magnetoresistance. The notion of an optimal triad enables us to fit the experimental data for the AHE to a functional dependence of the resistivity on magnetization given by Eq. (3.52). The agreement of the hopping pic-

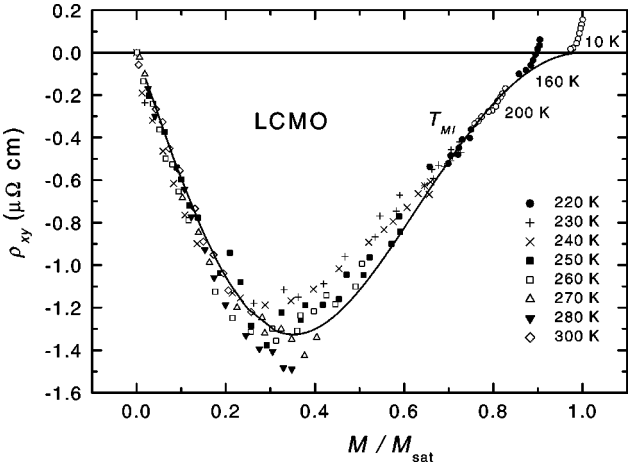

FIG. 18. Hall resistivity ρ_{xy} of LCMO versus reduced magnetization $M/M_{\rm sat}$ for the data shown in Fig. 4. Note the scaling behavior, i.e., the extent to which ρ_{xy} can be regarded as depending on T and B solely through $M/M_{\rm sat}$. The solid line is a fit to Eq. (3.52) with $\rho_{xy}^0 = -6.2\ \mu\Omega$ cm.

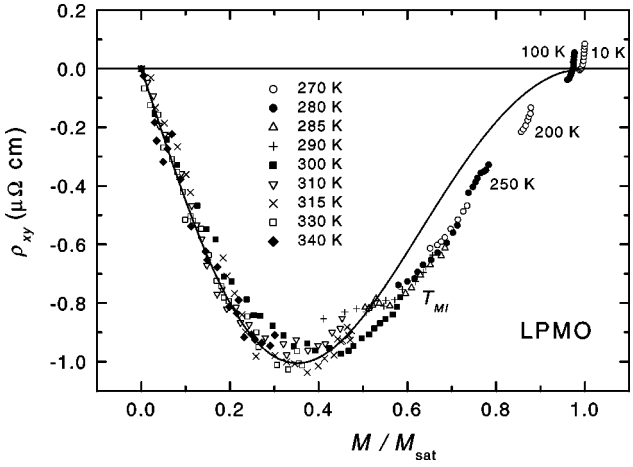

FIG. 19. Hall resistivity ρ_{xy} of LPMO versus reduced magnetization $M/M_{\rm sat}$ for the data shown in Fig. 5. Note the scaling behavior, i.e., the extent to which ρ_{xy} can be regarded as depending on T and B solely through $M/M_{\rm sat}$. The solid line is a fit to Eq. (3.52) with $\rho_{xy}^0 = -4.7\mu\Omega$ cm.

ture and experimental data in the transitional region is remarkable.

As we have mentioned above, the structure of the conducting network leading to the ordinary Hall effect in disordered doped semiconductors and the averaging procedures in these systems are still controversial.[76,75] In contrast to disordered doped semiconductors, manganites turn out to be systems in which the ability to tune average magnetization allows one to tune optimal triads, whose solid angles (the Pancharatnam phases) determine the AHE. The magnetization in manganites, therefore, serves as a scaling variable that has no analog in OHE in nonmagnetic disordered systems, and provides a check on our understanding of the conduction network. We note that the presence or absence of small polarons in the system does not change the scaling of the AHE resistivity, because, as follows from studies of polaronic transport in Refs. 35–37 and 76, Eq. (3.47) also holds for small polaron hopping.

IV. HALL RESISTIVITY: COMPARISON OF THEORY AND EXPERIMENT

The scaling of the Hall resistivity is shown in Figs. 18, 19, and 20, in which the data shown in Figs. 4, 5, and 6, respectively, are replotted as a function of $M/M_{\rm sat}$. At and above T_c the data fall on a smooth curve that reaches an extremum at $M/M_{\rm sat} \simeq 0.4$ for LSMO and LPMO and at $M/M_{\rm sat} \simeq 0.35$ for LCMO. Below T_c the data first change rapidly with magnetization as domains are swept from the sample before saturating and following the general trend. At the lowest temperatures, the metallic OHE appears as a positive contribution at constant magnetization. As for the magnitude of the Hall resistivity, for LPMO the solid curve in Fig. 19 follows Eq. (3.52) with $\rho_{xy}^0 = -4.7\ \mu\Omega$ cm is consistent with the estimates of ρ_{xx} and ρ_{xy} given above. Down to 285 K, which is the Curie temperature determined by scaling analysis, Eq. (3.50) describes the data for LPMO reasonably well. In addition, the extremum found from this equation is located at $M/M_{\rm sat} = \cos\beta \approx 0.35$, close to the experimental extremum.

In LCMO and LSMO, the agreement between theoretical and experimental results is good as well. We note that below T_c, the longitudinal resistivity is metallic and no longer dominated by magnetic disorder. We have not expected an agreement between theory and experiment in this range of temperatures, but in LCMO and LSMO scaling persists at temperatures below T_C, with notable exception of the range of low temperatures and magnetizations close to saturation value, where the ordinary Hall effect manifests itself. We note in this regard that below T_C, local spin arrangements still can still dominate the AHE via asymmetric scattering or side jumps. The numerator of Eq. (3.52), $m(1-m^2)^2$, which is characteristic for the behavior of σ_{xy} alone, has an extre-

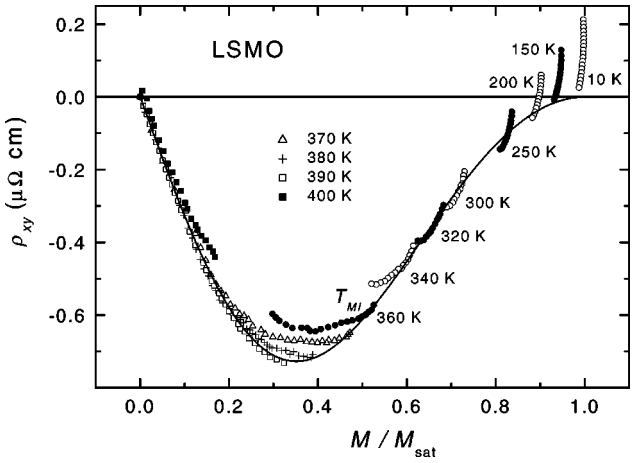

FIG. 20. Hall resistivity ρ_{xy} of LSMO versus reduced magnetization $M/M_{\rm sat}$ for the data shown in Fig. 5. Note the scaling behavior, i.e., the extent to which ρ_{xy} can be regarded as depending on T and B solely through $M/M_{\rm sat}$. The solid line is a fit to Eq. (3.52) with $\rho_{xy}^0 = -3.4\ \mu\Omega$ cm.

mum at $m=1/\sqrt{5}\approx 0.45$ as shown by the dashed line in Fig. 19. The broader maximum in the data suggest a shift toward a hopping model for ρ_{xx} and ρ_{xy} as the sample is warmed through the metal-insulator transition.

V. CONCLUSIONS

Our investigation of the Hall resistivity, the longitudinal resistivity, and the magnetization in single crystals of three different manganite compounds suggests that near and somewhat above the ferromagnet-to-paramagnet transition temperature, transport properties are determined by charge carrier hopping between localized states. We find both theoretically and experimentally that the Hall resistivity is solely determined by the sample magnetization (M) near and somewhat above the transition temperature. A microscopic model for the anomalous Hall effect based on the Holstein picture of the ordinary Hall effect in the hopping regime has been proposed and explains the results quite well. The anomalous Hall effect arises due to interference between direct hopping between two sites and hopping via a third site, with the quantal phase provided by topologically nontrivial configurations of Mn ion core spins in the presence of strong Hund's rule coupling. These force the hopping charge carrier to follow the local spin texture, with the average quantal phase arising due to local Pancharatnam phases and Dzyaloshinski-Moriya spin-orbit interactions. Below the transition temperature, the AHE competes with the OHE as long-range magnetic order and, presumably, an infinite percolating metallic cluster, develops.

ACKNOWLEDGMENT

We are grateful to I. L. Aleiner, D. P. Arovas, S. L. Cooper, E. Dagotto, S. Fishman, J. Lynn, A. J. Millis, V. L. Pokrovsky, H. Roder, and P. B. Wiegmann for useful discussions. This material is based upon work supported by the U.S. Department of Energy, Division of Materials Sciences under Grant No. DEFG02-96ER45439 through the University of Illinois Materials Research Laboratory. Additional support from NSF-DMR99-75187 is also gratefully acknowledged.

*Email address: lyandage@uiuc.edu

†Email address: schun@psu.edu. Present address: Department of Physics, Pennsylvania State University, University Park, PA 16802-6300.

‡Email address: salamon@uiuc.edu

§Email address: goldbart@uiuc.edu

[1] S. Jin, T. H. Tiefel, M. McCormack, R. A. Fastnacht, R. Ramesh, and J. H. Chen, Science **264**, 413 (1994).

[2] A. P. Ramirez, J. Phys.: Condens. Matter **9**, 8171 (1997).

[3] G. J. Snyder, M. R. Beasley, T. H. Geballe, R. Hiskes, and S. DiCarolis, Appl. Phys. Lett. **69**, 4254 (1996); G. J. Snyder, R. Hiskes, S. DiCarolis, M. R. Beasley, and T. H. Geballe, Phys. Rev. B **53**, 14 434 (1996).

[4] M. Jaime, H. T. Hardner, M. B. Salamon, M. Rubinstein, P. Dorsey, and E. Emin, Phys. Rev. Lett. **78**, 951 (1997).

[5] P. Wagner, D. Mazilu, L. Trappeniers, V. Moshchalkov, and Y. Bruynseraede, Phys. Rev. B **55**, R14 721 (1997).

[6] P. Matl, N. P. Ong, Y. F. Yan, Y. Q. Li, D. Studebaker, T. Baum, and G. Doubinina, Phys. Rev. B **57**, 10 248 (1998).

[7] G. Jakob, F. Martin, W. Westerburg, and H. Adrian, Phys. Rev. B **57**, 10 252 (1998); G. Jakob, W. Westerburg, F. Martin, H. Adrian, P. J. M. van Bentum, and J. A. A. J. Perenboom, J. Appl. Phys. **85**, 4803 (1999); W. Westerburg, F. Martin, G. Jakob, P. J. M. van Bentum, and J. A. A. J. Perenboom, cond-mat/9907346 (unpublished).

[8] A. Asamitsu and Y. Tokura, Phys. Rev. B **58**, 47 (1998).

[9] S. H. Chun, M. B. Salamon, and P. D. Han, Phys. Rev. B **59**, 11 155 (1999); J. Appl. Phys. **85**, 5573 (1999).

[10] S. H. Chun, M. B. Salamon, P. D. Han, Y. Lyanda-Geller, and P. M. Goldbart, Phys. Rev. Lett. **84**, 757 (2000).

[11] Y. Lyanda-Geller, P. M. Goldbart, S. H. Chun, and M. B. Salamon, cond-mat/9904331 (unpublished).

[12] S. H. Chun, M. B. Salamon, Y. Tomioka, and Y. Tokura, Phys. Rev. B **61**, R9225 (2000).

[13] See, e.g., N. F. Mott and H. S. W. Massey, *Theory of Atomic Collisions* (Clarendon, Oxford, 1965).

[14] J. Smit, Physica (Amsterdam) **23**, 39 (1958).

[15] J. Luttinger, Phys. Rev. **112**, 739 (1958).

[16] F. E. Maranzana, Phys. Rev. **160**, 421 (1967).

[17] L. Berger, Phys. Rev. B **2**, 4559 (1970).

[18] P. Nozières and C. Lewiner, J. Phys. (Paris) **34**, 901 (1973).

[19] Y. Lyanda-Geller, Pis'ma Zh. Éksp. Teor. Fiz. **46** 388 (1987) [JETP Lett. **46**, 489 (1987)].

[20] C. Zener, Phys. Rev. **82**, 403 (1951).

[21] P. W. Anderson and H. Hasegawa, Phys. Rev. **100**, 675 (1955).

[22] P. G. De Gennes, Phys. Rev. **118**, 141 (1960).

[23] T. Holstein, Phys. Rev. **124**, 1329 (1961).

[24] Y. Aharonov and D. Bohm, Phys. Rev. **115**, 485 (1959).

[25] S. Pancharatnam, Proc.-Indian Acad. Sci., Sect. A **44**, 247 (1956).

[26] M. V. Berry, J. Mod. Opt. **34**, 1401 (1987).

[27] I. E. Dzyaloshinski, J. Phys. Chem. Solids **4**, 241 (1958); T. Moriya, Phys. Rev. Lett. **4**, 5 (1960). For bandlike electrons terms of similar type were discussed in P. M. Levy and A. Fert, Phys. Rev. B **23**, 4667 (1981).

[28] Y. B. Kim, P. Majumdar, A. J. Millis, and B. I. Shraiman, cond-mat/9803350 (unpublished).

[29] J. Ye, Y. B. Kim, A. J. Millis, B. I. Shraiman, P. Majumdar, and Z. Tesanovic, Phys. Rev. Lett. **83**, 3737 (1999).

[30] Ye *et al.* (Ref. 29), in an attempt to describe transport at high temperatures, have invoked an expansion in powers of t/kT (i.e., the coherent hopping amplitude t divided by the temperature), and thereby have identified the familiar Berry-phase acquired during motion through a magnetic texture. Using this, they have discussed the AHE by inserting the resulting effective magnetic field originating from the Berry phase into the Drude-approach formula for the ordinary Hall coefficient. In this approach, the microscopic degrees of freedom leading to carrier localization are not treated explicitly, but instead are embodied by temperature; the carrier transport is addressed by considering the effective magnetic field due to spin texture.

[31] Y. Lyanda-Geller, P. M. Goldbart and I. L. Aleiner (unpublished).

[32] A. J. Millis, P. B. Littlewood, and B. I. Shraiman, Phys. Rev. Lett. **74**, 5144 (1995).

[33] C. M. Varma, Phys. Rev. B **54**, 7328 (1996).
[34] A. J. Millis, B. I. Shraiman, and R. Mueller, Phys. Rev. Lett. **77**, 175 (1996).
[35] T. Holstein, Ann. Phys. (N.Y.) **20**, 325 (1961).
[36] L. Friedman and T. Holstein, Ann. Phys. (N.Y.) **21**, 494 (1963).
[37] D. Emin and T. Holstein, Ann. Phys. (N.Y.) **53**, 439 (1969).
[38] L. Sheng, D. Y. Xing, D. N. Sheng, and C. S. Ting, Phys. Rev. Lett. **79**, 1710 (1997).
[39] A. Efros and B. Shklovskii, *Electronic Properties of Disordered Conductors* (Springer, New York, 1984).
[40] P. A. Lee and T. V. Ramakrishnan, Rev. Mod. Phys. **57**, 287 (1985).
[41] I. M. Lifshitz, Usp. Fiz. Nauk. **83**, 617 (1965) [Sov. Phys. Usp. **7**, 549 (1964)].
[42] V. Ambegaokar, B. I. Halperin, and J. S. Langer, Phys. Rev. B **4**, 2612 (1971).
[43] Y. Tomioka, A. Asamitsu, and Y. Tokura (unpublished).
[44] M. Jaime, P. Lin, M. B. Salamon, and P. D. Han, Phys. Rev. B **58**, R5901 (1998).
[45] S. H. Chun, M. B. Salamon, Y. Tomioka, A. Asamitsu, and Y. Tokura (unpublished).
[46] C. M. Hurd, *The Hall Effect in Metals and Alloys* (Plenum, New York, 1972).
[47] N. Nagaosa and P. A. Lee, Phys. Rev. Lett. **64**, 2450 (1990).
[48] L. B. Ioffe, V. Kalmeyer, and P. B. Wiegmann, Phys. Rev. B **43**, 1219 (1991).
[49] E. Müller-Hartmann and E. Dagotto, Phys. Rev. B **54**, 6819 (1996).
[50] Y. Lyanda-Geller, I. L. Aleiner, and P. M. Goldbart, Phys. Rev. Lett. **81**, 3215 (1998).
[51] Owing to the discreteness of the hopping, the quantal phases (Refs. 47–49) might more appropriately be termed Pancharatnam (rather than Berry) phases (Refs. 25 and 26).
[52] R. H. Heffner, J. E. Sonnier, D.E. MacLaughlin, G. J. Niewenhuys, G. Ehlers, F. Mezei, S-W. Cheong, J. S. Gardner, and H. Röder (unpublished).
[53] M. Lau and C. Dasgupta, Phys. Rev. B **39**, 7212 (1989).
[54] See, e.g., N. Furukawa, J. Phys. Soc. Jpn. **63**, 3214 (1994).
[55] E. Abrahams, P. W. Anderson, D. C. Licciardello, and T. V. Ramakrishnan, Phys. Rev. Lett. **42**, 673 (1979).
[56] A. Mackinnon and B. Kramer, Phys. Rev. Lett. **47**, 1546 (1981).
[57] It was also demonstrated by M. Kamal and G. Murthy [Phys. Rev. Lett. **71**, 1911 (1993)] that suppression (absence) of hedgehogs results in a phase transition which characteristics (exponents) are different from those in the Heisenberg model.
[58] A. Miller and E. Abrahams, Phys. Rev. **120**, 745 (1960).
[59] D. Louca, T. Egami, E. L. Brosha, H. Roder, and A. R. Bishop, Phys. Rev. B **56**, R8475 (1997).
[60] S. J. L. Billinge, R. G. DiFranchesko, G. H. Kwei, J. J. Neumeier, and J. D. Thompson, Phys. Rev. Lett. **77**, 715 (1996).
[61] J. Lynn, R. Ervin, J. Borching, Q. Huang, A. Santoro, J. Peng, and Z. Li, Phys. Rev. Lett. **76**, 4046 (1996).
[62] G. M. Zhao, K. Conder, H. Keller, and K. A. Muller, Nature (London) **381**, 676 (1996); G. M. Zhao, M. B. Hunt, and H. Keller, Phys. Rev. Lett. **78**, 955 (1997); J. P. Franck, I. Isaak, W. M. Chen, J. Chrzanovski, and J. C. Irwin, Phys. Rev. B **58**, 5189 (1998); A. M. Balagurov, V. Y. Pomjakushin, D. V. Speptyakov, V. L. Aksenov, N. A. Babushkina, L. M. Belova, A. N. Taldenkov, A. V. Iluyshkin, P. Fisher, M. Guttman, L. Keller, O. Y. Gorbenko, and A. R. Kaul, *ibid.* **60**, 383 (1999).
[63] T. G. Perring, G. Aeppli, S. M. Hayden, S. A. Carter, J. P. Remeika, and S. W. Cheong, Phys. Rev. Lett. **77**, 711 (1996).
[64] M. Jaime, P. Lin, S. H. Chun, M. B. Salamon, P. Dorsey, and M. Rubinstein, Phys. Rev. B **60**, 1028 (1999).
[65] J. Fontcuberta, A. Seffar, X. Granados, J. L. Garsia J. Munoz, X. Obradors, and S. Pinol, Appl. Phys. Lett. **68**, 2288 (1996).
[66] S. Yoon *et al.*, Phys. Rev. B **58**, 2795 (1998).
[67] R. D. Merithew, M. B. Weismann, F. M. Hess, P. Spradling, E. R. Nowak, J. O'Donnel, J. N. Eckstein, Y. Tokura, and Y. Tomioka, Phys. Rev. Lett. **84**, 3442 (2000).
[68] See, e.g., J. M. Ziman, *Elements of Advanced Quantum Theory* (London, Cambridge University, 1969), Sec. 3.1.
[69] W. Schirmacher, Phys. Rev. B **41** 2461 (1990).
[70] The essential product of three overlap integrals, sensitive to magnetic flux through loops of nonzero area, $V_{hk}V_{kj}V_{jh}$, can enter the transition rate also through the energy denominators, as we have invoked Brillouin-Wigner rather than Rayleigh-Schrödinger perturbation theory. However, the corresponding contributions to the probability is of the higher order in powers of small parameter of our perturbation expansion, $V_{ij}/(E_i - E_j)$, than terms features in Eq. (3.14).
[71] B. I. Shklovskii and B. Z. Spivak, in *Hopping Transport in Solids*, edited by M. Pollak and B. Shklovskii (Elsevier Science, New York, 1991), p. 271.
[72] By two-phonon process (assisting the Hall effect) we mean one involving probabilities (computed in perturbation theory) characterized by four carrier-phonon interaction vertices; the probability of a single-phonon process (leading to the longitudinal conductivity) involves two such vertices.
[73] As was discussed by Holstein, strictly speaking, there exists a possibility of obtaining an imaginary denominator in two-phonon processes, in which an additional δ function does not appear, but, for example, energies of two unoccupied states in a triad are in resonance allowing elastic transition. However, the possibility that two unoccupied states will be in resonance is negligibly small in a disordered strongly correlated system.
[74] It is interesting to mention that although in contributions involving three-stage processes only one phonon mode changes its population, both (i) and (ii) have similar temperature dependence: the contribution involving interference of one and three-stage processes is proportional to both the population factor of the phonon mode which changes its population, and to the population of the phonon mode which population is not changed (this mode is involved on the intermediate site).
[75] Y. M. Galperin, E. P. German, and V. G. Karpov, Zh. Éksp. Teor. Fiz. **99**, 343 (1991) [Sov. Phys. JETP **72**, 193 (1991)].
[76] O. Entin-Wohlman, A. G. Aronov, and Y. Levinson, Y. Imry, Phys. Rev. Lett. **75**, 4094 (1995).
[77] In the context of high temperature superconductors, OH current noise has been considered by L. Ioffe, G. Lesovik, and A. J. Millis, Phys. Rev. Lett. **77**, 1584 (1996). The spin quantal phase accrued by hopping carriers on plaquettes of ions with disordered spins in high temperature superconductors, was also shown to affect the ordinary Hall effect (Ref. 48).
[78] See, e.g., A. Goldhaber, Phys. Rev. Lett. **62**, 482 (1989).
[79] M. R. Ibarra and J. M. De Teresa, in *Colossal Magnetoresistance, Charge Order and Related Phenomena*, edited by C. N. Rao and R. Raveau (World Scientific, Singapore, 1998).

[80] I. F. Lyuksytov and V. L. Pokrovsky, Mod. Phys. Lett. B **13**, 379 (1999).
[81] Z. Popovich and S. Satpathy, Phys. Rev. Lett. **84**, 1603 (1999).
[82] L. D. Landau and E. M. Lifshitz, *Quantum Mechanics* (Pergamon, Oxford, 1977).